Alcohol modulation of BK channel gating depends on β subunit composition

Guruprasad Kuntamallappanavar and Alex M. Dopico

Department of Pharmacology, College of Medicine, The University of Tennessee Health Science Center, Memphis, TN 38103

In most mammalian tissues, Ca^{2+}_i/voltage-gated, large conductance K^+ (BK) channels consist of channel-forming slo1 and auxiliary (β1–β4) subunits. When Ca^{2+}_i (3–20 µM) reaches the vicinity of BK channels and increases their activity at physiological voltages, β1- and β4-containing BK channels are, respectively, inhibited and potentiated by intoxicating levels of ethanol (50 mM). Previous studies using different slo1s, lipid environments, and Ca^{2+}_i concentrations—all determinants of the BK response to ethanol—made it impossible to determine the specific contribution of β subunits to ethanol action on BK activity. Furthermore, these studies measured ethanol action on ionic current under a limited range of stimuli, rendering no information on the gating processes targeted by alcohol and their regulation by βs. Here, we used identical experimental conditions to obtain single-channel and macroscopic currents of the same slo1 channel ("cbv1" from rat cerebral artery myocytes) in the presence and absence of 50 mM ethanol. First, we assessed the role five different β subunits (1,2,2-IR, 3-variant d, and 4) in ethanol action on channel function. Thus, two phenotypes were identified: (1) ethanol potentiated cbv1-, cbv1+β3-, and cbv1+β4-mediated currents at low Ca^{2+}_i while inhibiting current at high Ca^{2+}_i, the potentiation–inhibition crossover occurring at 20 µM Ca^{2+}_i; (2) for cbv1+β1, cbv1+wt β2, and cbv1+β2-IR, this crossover was shifted to ∼3 µM Ca^{2+}_i. Second, applying Horrigan–Aldrich gating analysis on both phenotypes, we show that ethanol fails to modify intrinsic gating and the voltage-dependent parameters under examination. For cbv1, however, ethanol (a) drastically increases the channel's apparent Ca^{2+} affinity (nine-times decrease in K_d) and (b) very mildly decreases allosteric coupling between Ca^{2+} binding and channel opening (C). The decreased K_d leads to increased channel activity. For cbv1+β1, ethanol (a) also decreases K_d, yet this decrease (two times) is much smaller than that of cbv1; (b) reduces C; and (c) decreases coupling between Ca^{2+} binding and voltage sensing (parameter E). Decreased allosteric coupling leads to diminished BK activity. Thus, we have identified critical gating modifications that lead to the differential actions of ethanol on slo1 with and without different β subunits.

INTRODUCTION

Large conductance, Ca^{2+}- and voltage-gated K^+ (BK) channels are widely expressed in both excitable and nonexcitable tissues and thus play a critical role in several physiological processes, such as neurotransmitter release, hormone secretion, circadian rhythms, inflammatory responses, metastasis progression, and regulation of smooth muscle tone (Weiger et al., 2002; Lu et al., 2006; Salkoff et al., 2006; Dopico et al., 2012). Functional BK channels result from tetrameric association of channel-forming α subunits (encoded by the *Slo1* or *KCNMA1* gene), which are often referred to as slo1 channels. Each slo1 subunit consists of a transmembrane "core" (S0–S6) and a long cytosolic domain (CTD). In most mammalian tissues, however, slo1 proteins are associated with auxiliary β1–β4 subunits (encoded by *KCNMB1–4*; Knaus et al., 1994; Wallner et al., 1999; Xia et al., 1999; Behrens et al., 2000; Brenner et al., 2000a; Uebele et al., 2000). Unlike α subunits, BK β subunits do not form functional channels themselves. Rather, they usually alter several gating processes, which leads to modification of the channel's response to physiological ligands, such as Ca^{2+}_i, and/or changes in macroscopic current kinetics (McManus et al., 1995; Brenner et al., 2000a; Cox and Aldrich, 2000; Nimigean and Magleby, 2000; Qian and Magleby, 2003; Orio and Latorre, 2005). For example, β1 subunit–induced changes in gating include modifications in intrinsic gating (i.e., gating in the absence of activating Ca^{2+}_i/voltage; Bao and Cox, 2005; Gruslova et al., 2012), stabilization of the slo1 voltage sensor in the active configuration (Bao and Cox, 2005; Contreras et al., 2012; Castillo et al., 2015), increased affinity for Ca^{2+} in the RCK1 domain high-affinity Ca^{2+}-sensing site when the channel is open, decreased affinity for Ca^{2+} in the RCK2 domain Ca^{2+}-sensing site when the channel is closed (Bao and Cox, 2005; Sweet and Cox, 2009), and increased allosteric coupling between Ca^{2+} binding and channel opening (reviewed in Hoshi et al. [2013]) while not modifying equivalent gating charge (Bao and Cox, 2005; Contreras et al., 2012; Castillo et al., 2015). The β1-dependent gating modifications lead to a signif-

Correspondence to Alex M. Dopico: adopico@uthsc.edu

Abbreviations used: CTD, cytosolic domain; HA, Horrigan–Aldrich; I/O, inside-out; wt, wild type.

The Rockefeller University Press $30.00
J. Gen. Physiol. 2016 Vol. 148 No. 5 419–440
https://doi.org/10.1085/jgp.201611594

icant increase in the channel's apparent binding affinity for Ca^{2+}_i, which is evident by a decrease in the voltage needed for reaching half-value in the conductance (G)/maximal conductance plot ($V_{0.5}$) when ionic current behavior is evaluated at ≥1 µM Ca^{2+}_i (Cox and Aldrich, 2000).

It is noteworthy that the expression of the different *KCNMB* transcripts is highly tissue specific: thus, β1 mRNA is particularly abundant in vascular and nonvascular smooth muscle (Nelson and Quayle, 1995; Brenner et al., 2000b), wild-type (wt) β2 is the predominant transcript in adrenochromaffin cells (Wallner et al., 1999; Xia et al., 1999), β3 is abundant in testis, pancreas, skeletal muscle, and spleen (Behrens et al., 2000; Brenner et al., 2000a; Uebele et al., 2000), and β4 is abundant in central neurons (Behrens et al., 2000; Brenner et al., 2000a). Distinct expression patterns from one tissue to another may enable a given β subunit type to contribute to physiology in a tissue-specific manner. For example, β1 subunits are critical to fine tune the overall Ca^{2+} sensitivity of the BK channel complex (Brenner et al., 2000a; Cox and Aldrich, 2000), allowing channel activation by low µM Ca^{2+}, which is reached in the vicinity of the BK channel during depolarization-induced myocyte contraction (Pérez et al., 2001). Local Ca^{2+} levels are usually generated by local signals termed "Ca^{2+} sparks," which result from the activity of ryanodine receptors in the sarcoplasmic reticulum (Jaggar et al., 2000; Ledoux et al., 2006). Functional coupling between Ca^{2+} sparks and plasma membrane BK channels via β1 subunits generates outward K^+ current in the vascular myocyte, which opposes depolarization-induced Ca^{2+} influx and smooth muscle contraction (Brenner et al., 2000b). Indeed, *KCNMB1* knockout mice characteristically suffer from reduced spark–BK coupling and BK-mediated current in vascular smooth muscle (Brenner et al., 2000b).

Ethanol concentrations obtained in blood during moderate to heavy alcohol intoxication (50 mM) drastically modulate BK channel open probability (Po) and, thus, macroscopic current (Brodie et al., 2007; Martin et al., 2008; Wynne et al., 2009). The final effect of ethanol on BK channel currents depends on a variety of factors (reviewed in Brodie et al. [2007] and Dopico et al. [2014]), including posttranslational modification of slo1 proteins (Liu et al., 2006; Palacio et al., 2015), levels of Ca^{2+}_i (Liu et al., 2008), and the lipid environment of the BK channel complex, in particular, cholesterol levels (Crowley et al., 2003; Yuan et al., 2011) and type of phospholipid species (Crowley et al., 2005; Yuan et al., 2011) in the lipid bilayer where the slo1 channel resides. Several studies have documented different outcomes when ethanol action is evaluated on BK channels of different subunit composition, including homomeric slo1, slo1+β1, and slo1+β4; potentiation, inhibition, and ethanol refractoriness have all been reported (Crowley et al., 2003, 2005; Liu et al., 2004, 2008, 2013; Martin et al., 2008; Bukiya et al., 2009a). The use of different slo1 subunits, channel expression systems, lipid bilayer composition, and activating Ca^{2+} levels in these previous studies makes it impossible to address the precise contribution of regulatory β subunits to ethanol action on BK channels. Filling this knowledge gap acquires particular relevance because ethanol action on BK channels appears to be β subunit dependent; at physiological Ca^{2+}_i levels, neuronal and recombinant (slo1 and slo1+β4) channels are usually activated by ethanol, whereas vascular smooth muscle and recombinant slo1+β1 are usually inhibited (reviewed in Dopico et al. [2014]). The relevance of this topic is compounded by the fact that differential actions of ethanol on BK channels have a direct impact on tissue physiology: ethanol (40–50 mM) activation of native BK channels thought to consist of α and/or α+β4 subunits leads to reduced action potential (AP) firing rate and neuronal excitability, as reported for nucleus accumbens medium spiny neurons (Martin et al., 2004, 2008) and dorsal root ganglia nociceptive neurons (Gruß et al., 2001). In contrast, inhibition of smooth muscle BK channels by 10–100 mM ethanol leads to cerebral artery constriction. Moreover, genetic ablation of BK β1 subunits totally blunts this alcohol action (Liu et al., 2004; Bukiya et al., 2009a).

Another major gap in the current knowledge on ethanol–BK channel interactions results from the fact that all previous studies have evaluated ethanol action on steady-state macroscopic current and/or steady-state single-channel open probability (Po; reviewed in Brodie et al. [2007] and Dopico et al. [2014]). This descriptive approach falls short of identifying the gating mechanisms targeted by ethanol, which leads to ethanol-induced perturbation of BK current and possible dependence on the different regulatory β subunits.

In this study, we combined patch-clamp electrophysiology and analysis of BK channel gating by using an allosteric model to (a) determine the distinct contribution of each β subunit type to ethanol action on BK channels and (b) identify the gating mechanisms targeted by ethanol and their modulation by BK β subunits. Thus, we expressed the same slo1 isoform (cbv1) alone or with β1, wt β2, and β2 with its NH_2 end deleted to remove inactivation (β2-IR), β3 (d variant), or β4 and obtained single-channel or macroscopic current recordings in the absence and presence of intoxicating levels of ethanol (50 mM) across a wide range of Ca^{2+}_i (0–100 µM). Then, data were fitted with the Horrigan–Aldrich (HA) allosteric model of BK channel gating. Our study demonstrates that (a) ethanol differentially modulates BK currents that result from channel complexes containing different β subunits under identical recording conditions and using the same slo1 channel. At physiological levels of Ca^{2+}_i, two phenotypes are revealed: slo1

like, which includes slo1+β3 and slo1+β4 channels, and slo1+β1 like, which includes slo1+wt β2 and slo1+β2-IR, the former phenotype being activated and the latter inhibited by ethanol. We also demonstrate that (b) ethanol action on BK channels is allosterically coupled to Ca^{2+}-driven gating and (c) both qualitative and quantitative differences in ethanol action on specific gating parameters contribute to the differential overall effect of ethanol (activation vs. inhibition) on BK channels when evaluated within physiological levels of Ca^{2+}_i.

MATERIALS AND METHODS

Expression of recombinant BK channel subunits

cDNA coding for BK channel–forming α subunits (cbv1; AY330293; the protein product has a 99% primary sequence conservation with the mslo1 mbr5 variant, NCBI) and β1 were cloned from rat cerebral artery myocytes as described previously (Jaggar et al., 2005; Liu et al., 2006). cbv1 cDNA was cleaved from the pBlueScript cloning vector by BamHI (Invitrogen) and XhoI (Promega) and directly reinserted into pOX vector for expression in *Xenopus laevis* oocytes. Linearization of pOX-cbv1 was done with NotI (Promega) and transcribed in vitro by using T3 polymerase. BK β1 subunit cDNA inserted into the EcoRI–SalI sites of the pCI-neo vector was linearized with NotI and transcribed in vitro by using T7 polymerase. Human wt β2 cDNA in pXMX vector and hβ3d in pCAP vector were gifts from C. Lingle (Washington University School of Medicine, St. Louis, MO). These plasmids were linearized with MluI (Invitrogen) and transcribed with T7. β2 subunit with the inactivation ball removed (β2-IR), β3 (human d variant), and human β4 were gifts from L. Toro (University of California, Los Angeles, Los Angeles, CA). β2-IR in pXMX vector was linearized with NotI and transcribed with T7. β3 cDNA inserted into the pOX vector was linearized with SalI (Invitrogen) and transcribed with T7. β4 cDNA was subcloned into pOX vector and linearized by NotI and transcribed using T3. In all cases, the mMES SAGE-mMACHINE kit (Ambion) was used for in vitro transcription. All cDNA sequences were confirmed by automatic sequencing at the University of Tennessee Health Science Center Molecular Research Center.

Care of animals and experimental protocols were reviewed and approved by the Institutional Animal Care and Use Committee at the University of Tennessee Health Science Center, an Association for Assessment and Accreditation of Laboratory Animal Care–accredited institution. Oocytes were removed from *Xenopus* (*Xenopus* Express) and prepared as described elsewhere (Dopico et al., 1998). cRNA was dissolved in diethyl polycarbonate–treated water at 50 (cbv1) and 150 (β1–4) ng/μl, with 1-μl aliquots being stored at −80°C. cbv1 cRNA (2.5–10 ng/μl) was coinjected with β1, wt β2, β2-IR, β3, or β4 (7.5–30 ng/μl) cRNA, giving β/cbv1 molar ratios ≥6:1 to ensure that all cbv1 subunits were saturated with βs (Dopico, 2003; Liu et al., 2013). cRNA injection (23–46 nl/oocyte) was performed using an automated nanoinjector (Drummond Scientific Co.). The interval between injection and patch-clamp recordings was 48–72 h.

Detection of coexpression of cbv1 and β3d proteins on the cell membrane surface by biotinylation and Western blotting

The presence of cbv1 and β3d proteins on the membrane surface of *Xenopus* oocytes was verified by biotinylation, using the Pierce Cell Surface Protein Isolation kit (Thermo Fisher Scientific) and following the manufacturer's instructions. Immediately before the biotinylation-based labeling and separation of membrane surface proteins, the oocyte's follicular layer was removed to allow access of kit reagents to the cell membrane. The purified surface protein fraction was analyzed by Western blotting, as follows.

Purified surface protein fraction for biotinylation (50 μg/lane) was separated on a 4–15% SDS–polyacrylamide gel and transferred onto polyvinylidene difluoride (PVDF) membranes. The membranes were then blocked with 5% nonfat dry milk made in Tris-buffered saline (TBS) containing 0.1% Tween 20 for 2 h. Membranes were then incubated with appropriate primary antibodies overnight at 4°C in TBS with 0.1% Tween 20 (TBS-T) and 5% nonfat dry milk. Membranes were then incubated with appropriate horseradish peroxidase–conjugated secondary antibodies (1:10,000 dilution; EMD Millipore) for 1–2 h at room temperature. Proteins were then visualized using the SuperSignal West Pico Chemiluminescent Substrate kit (Thermo Fisher Scientific). A mouse monoclonal anti-*KCNMB3* antibody (1:500 dilution; ab57219; Abcam) and mouse monoclonal anti-slo1 antibody (1:1,000 dilution; University of California, Davis/National Institutes of Health NeuroMab) were used to detect β3d and cbv1 proteins, respectively.

Electrophysiology

After oocyte preparation for patch-clamp electrophysiology, either single-channel or macroscopic currents were recorded from inside-out (I/O) patches, as previously described (Dopico, 2003; Liu et al., 2008; Kuntamallappanavar et al., 2014). Both bath and electrode solutions contained (mM) 135 K^+ gluconate, 5 EGTA, 2.28 $MgCl_2$, 15 HEPES, and 1.6 HEDTA, pH 7.4. In all experiments, the desired free $[Ca^{2+}]_i$ was obtained by adding $CaCl_2$, with free Mg^{2+} being kept constant at 1 mM. Free Ca^{2+}_i and Mg^{2+} were calculated with MaxChelator (WEBMAXC; Stanford University) and validated experimentally using Ca^{2+}_i-selective and reference electrodes (Corning) as described elsewhere (Dopico, 2003). For experiments in nominal zero Ca^{2+}_i, Ca^{2+} buff-

ering was achieved by including 10 mM EGTA in the solution; neither Ca^{2+}_i nor HEDTA was added to this solution. Free $[Ca^{2+}]_i$ in this nominal zero Ca^{2+}_i solution is ~0.5 nM (Cox and Aldrich, 2000).

Patch-recording electrodes were pulled from glass capillaries and treated as described previously (Dopico et al., 1998). When filled with high K^+ solution (see above composition of electrode solution), the vast majority of tip resistances were ~2 MΩ, with a few reaching 5 MΩ. Series resistance was electronically compensated up to 80% by the EPC8 amplifier. An Ag/AgCl electrode with gluconate as main anion was used as ground electrode. Experiments were performed at room temperature (20–22°C).

Macroscopic currents were evoked from I/O macropatches held at −80 mV by 100-ms-long, 10-mV depolarizing steps from −150 to 150–200 mV. A P/4 leak subtraction routine was applied using a built-in function in pCLAMP. Currents at single-channel resolution were acquired from I/O patches in gap-free recording at V_m = −20 to −40 mV for 30 s under each experimental condition. Data were acquired using an EPC8 amplifier (HEKA), low-passed at 1 kHz by using an eight-pole Bessel filter (902LPF; Frequency Devices), and digitized at 5 kHz by using a Digidata 1320A A/D converter and pCLAMP 8.0 (Molecular Devices). For HA analysis, data were low-pass filtered at 10 kHz and sampled at 50 kHz. The number of channels in the patch (N) was estimated by switching the perfusion solution from nominal zero Ca^{2+}_i to ≥10 µM Ca^{2+}_i, which drives the individual opening probability (Po) close to unity, and then measuring peak macroscopic current amplitude (I) size and unitary current amplitude (i) at 20–90 mV. Thus, N = I/i. As an index of channel steady-state activity, we used the product NPo, which was obtained using a built-in option in Clampfit 9.2 (Molecular Devices) from ≥30 s of continuous recording under each experimental condition. This built-in algorithm uses a half-amplitude threshold method for event detection.

Fitting data to the HA model

According to this model, Po at any voltage and Ca^{2+}_i concentration is given by the following equation (Horrigan and Aldrich, 1999, 2002; Horrigan et al., 1999):

$$Po = \frac{L(1+JD+KC+JKCDE)^4}{L(1+JD+KC+JKCDE)^4+(1+JK+JKE)^4}, \quad (1)$$

where

$$\begin{aligned} J &= \exp\left[\frac{z_J F(V-V_h(J))}{RT}\right] \\ K &= \frac{[Ca^{2+}]}{K_d} \\ L &= L_0 \exp\left(\frac{z_L FV}{RT}\right). \end{aligned} \quad (2)$$

In the absence of Ca^{2+}_i, the probability of channel opening as a function of voltage is given by the equation

$$Po = \left[1+\frac{(1+J)^4}{L(1+JD)^4}\right]^{-1}. \quad (3)$$

In contrast, in the absence of voltage sensor activation, Ca^{2+}_i binding strongly affects channel opening (Horrigan and Aldrich, 2002; Sweet and Cox, 2008, 2009). In addition, Po is very small at extreme negative voltages. Thus, Po can be expressed as

$$Po = L\left[\frac{(1+KC)^4}{(1+K)^4}\right]. \quad (4)$$

According to Horrigan and Aldrich (2002), to determine K_d and C independently of N, the ratio (R_0) of NPo in the presence and absence of Ca^{2+} was obtained from

$$\begin{aligned} R_0\left([Ca^{2+}]\right) &= \frac{NPo[V,[Ca^{2+}]]}{NPo[V,0]} \\ &= \left[\frac{1+KC}{1+K}\right]^4 = \left[\frac{1+C[Ca^{2+}]/K_d}{1+[Ca^{2+}]/K_d}\right]^4, \end{aligned} \quad (5)$$

where L_0 = closed to open conformation equilibrium constant at V = 0, and no Ca^{2+}_i bound to the channel; z_L = gating charge associated with channel opening; $V_h(J)$ = voltage at which the voltage sensors are half the time active when the channel is closed; z_J = gating charge associated with each voltage sensor's movement; K_d = dissociation constant when the channel is closed and all voltage sensors are in the resting state; C = allosteric coupling factor between Ca^{2+}_i binding and channel opening; D = allosteric coupling factor between voltage sensor activation and channel opening; E = allosteric coupling factor between Ca^{2+}_i binding and voltage sensor activation; R_0 = the NPo ratio in the presence and absence of Ca^{2+}_i and independent of L and N (see above). Therefore, R_0 depends only on K_d and C (Horrigan and Aldrich, 2002). In Eqs. 1, 2, 3, 4, and 5, R, T, and F have their usual meaning.

Chemicals and drug perfusion

Unless indicated otherwise, all chemicals were purchased from Sigma-Aldrich. On the day of the experiment, ethanol (100% purity; American Bioanalytical) was freshly added to the bath solution immediately before recordings. After excision from the cell, the cytosolic side of the membrane patch was exposed to a bath solution delivered from a pressurized, automated DAD12 system (ALA Scientific Instruments) via a micropipette tip having an internal diameter of 100 µm. Bath solution with urea isoosmotically substituting for ethanol was used as control perfusion, with osmolarity of all solutions ranging from 301 to 322 mOsM (Wescor Vapro).

Data analysis

Electrophysiology data were analyzed with pCLAMP 9.2 (Molecular Devices). G (conductance)/G_{max}-V curves obtained from macroscopic ionic current at steady-state

level were fitted to a Boltzmann function of the type $G(V) = G_{max}/(1 + \exp[-V + V_{0.5})k])$. Boltzmann-fitting routines were run using a Levenberg–Marquardt algorithm to perform nonlinear least squares fits. From G/G_{max}-V plots, we obtained the voltage required to achieve half-maximal conductance ($V_{0.5}$). For inactivating currents (cbv1+wt β2), $V_{0.5}$ was determined from the peak current immediately before the onset of inactivation. Macroscopic current activation and deactivation data were fitted to standard exponential functions using a Chebyshev approximation. Time constant for current activation (τ_{act}) was measured at the voltage at which the channel reached maximal steady-state activity (V_{max}), whereas the deactivation time constant (τ_{deact}) was measured after voltage reached V_{max} and then stepped down to −80 mV (Kuntamallappanavar et al., 2014). Further analysis, plotting, and fitting were conducted using Origin 8.5 (OriginLab) and InStat 3.0 (GraphPad Software). Data are expressed as mean ± SEM; *n* = number of patches. Each patch was obtained from a different oocyte. Fitted parameters are expressed as mean ± 95% confidence intervals. Statistical analysis was conducted using Student's paired *t* test to compare the paired dataset (for instance, data before and after ethanol treatment). Multiple sets of data were compared using one-way ANOVA followed by Tukey's multiple comparison test (Glantz, 2001) to determine statistical significance of differences between individual means; significance was set at $P < 0.05$.

Online supplemental material

Fig. S1 demonstrates the surface expression of β3 variant d and the single-channel phenotype that results from coexpressing cbv1 with this β subunit. Fig. S2 shows ethanol's lack of effect in channels gated by voltage-Mg^{2+}_i in the absence of Ca^{2+}_i. Fig. S3 shows ethanol action on macroscopic currents originated from cbv1+wt β2.

RESULTS

Coexpression of different auxiliary β subunits with slo1 cloned from cerebral artery myocytes renders different macroscopic current phenotypes

Before probing ethanol on BK channels of different subunit composition (cbv1±βs), we assessed functional coexpression of the different β subunits (β1, wt β2, β2-IR, β3 variant d, and β4) with the channel-forming cbv1 subunit. Thus, using the oocyte expression system, macroscopic recordings were obtained from I/O patches over a wide range of Ca^{2+}_i concentrations (nominal zero to 100 µM). To identify the ion current phenotype from the different BK channel complexes, we obtained G/G_{max}-V plots according to well-established acquisition voltage protocols (see Materials and methods). Representative ionic currents obtained at 10 µM free Ca^{2+}_i are shown in Fig. 1 A. From G-V plots, we obtained the voltage required to achieve half-maximal conductance ($V_{0.5}$) and, eventually, $V_{0.5}$-$[Ca^{2+}]_i$ plots. From each macroscopic ionic current recording, time constants for current activation (τ_{act}) and deactivation (τ_{deact}) were measured as stated in Materials and methods.

β1 subunits increased cbv1 macroscopic current as Ca^{2+}_i was raised above micromolar levels. This is evident as a decrease in $V_{0.5}$ in the $V_{0.5}$-Ca^{2+} plot. Moreover, these plots show that the decrease in $V_{0.5}$ evoked by the presence of β1 becomes progressively larger as Ca^{2+} increases (Fig. 1 B). These results are in agreement with previously published data from BK complexes made of slo1+β1 other than cbv1 (Brenner et al., 2000a; Cox and Aldrich, 2000; Bao and Cox, 2005; Orio and Latorre, 2005; Contreras et al., 2012). The shift in $V_{0.5}$ has been widely conceptualized as a β1 subunit–induced increase in the apparent Ca^{2+}_i sensitivity of BK channel. In addition, β1 increased τ_{act} and τ_{deact} from their cbv1 values: 1.40 ± 0.10 and 1.13 ± 0.13 ms to 5.16 ± 0.93 and 6.76 ± 0.67 ms; all values were obtained at 10 µM Ca^{2+}_i ($P < 0.05$ for both constants; Fig. 1, C and D). This slowing down of macroscopic cbv1 current activation and deactivation kinetics by BK β1 subunits is also in accordance with data from slo1 other than cbv1 (Brenner et al., 2000a; Cox and Aldrich, 2000; Bao and Cox, 2005; Contreras et al., 2012). Therefore, macroscopic currents obtained from coexpression of β1 with cbv1 display a current phenotype characteristic of slo1+β1 currents.

When compared with β1, wt β2 subunits possess an additional inactivation domain in their N terminus (Wallner et al., 1995, 1999; Xia et al., 1999, 2003; Uebele et al., 2000). Indeed, coexpression of wt β2 with cbv1 channels consistently rendered macroscopic ionic currents that displayed fast inactivation (Fig. 1 A, bottom left). This result matches findings from other groups that coexpressed wt β2 with slo1 other than cbv1 (Wallner et al., 1999; Xia et al., 1999, 2003; Uebele et al., 2000). In contrast to wt β2, β2-IR has been engineered to lack the inactivation domain (Brenner et al., 2000a; Orio and Latorre, 2005; Sun et al., 2013). As found with β1 subunits, coexpression of β2-IR with cbv1 resulted in an increase of the channel's apparent Ca^{2+}_i sensitivity (Fig. 1 B). In addition, when compared with homomeric cbv1 channels, β2-IR–containing BK complexes rendered macroscopic ionic currents with very slow activation and deactivation kinetics: at 10 µM Ca^{2+}_i, τ_{act} and τ_{deact} changed from cbv1 values of 1.40 ± 0.10 and 1.13 ± 0.13 ms to 4.73 ± 0.74 and 6.22 ± 0.82 ms ($P < 0.05$ for both constants; Fig. 1, C and D). These cbv1+β2-IR versus cbv1 comparisons are consistent with previous data obtained by expressing β2-IR with slo1s other than cbv1 (Brenner et al., 2000a; Orio and Latorre, 2005; Sun et al., 2013).

In contrast to all other β subunits (including β4; see below in this paragraph), functional coexpression of

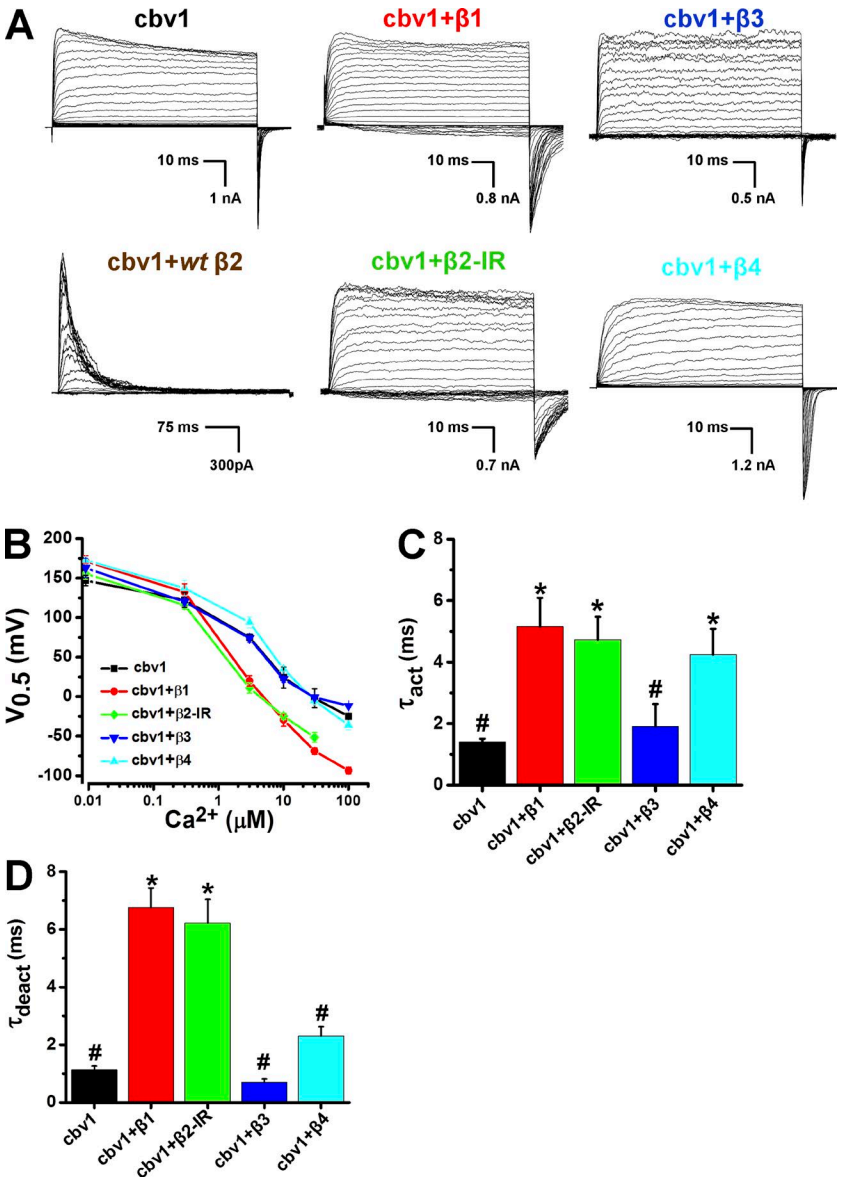

Figure 1. **Macroscopic currents recorded after cbv1+β1–4 subunit expression in *Xenopus* oocytes show characteristic features of BK currents.** (A) Representative current records from I/O macropatches expressing different BK channel subunit combinations (cbv1±β1/wt β2/β2-IR/β3/β4; 10 µM Ca^{2+}_i). Currents were evoked by 100 ms-long (except for cbv1+wt β2; 600 ms-long; 3 µM Ca^{2+}_i), 10-mV depolarizing steps from −150 to 150 mV, with a holding potential set to −80 mV. cbv1+wt β2 channels are characterized by fast inactivation. (B) $V_{0.5}$ versus $[Ca^{2+}]_i$ plot underscores that β subunit types differentially modulate the apparent Ca^{2+}_i sensitivity of the channel complex. (C and D) Bar graphs show averaged activation (τ_{act}) and deactivation (τ_{deact}) time constants, respectively, obtained at V_{max} with Ca^{2+}_i = 10 µM. Mean V_{max} (mV) values for different constructs were (mean ± SEM) cbv1 = 117 ± 8.2; cbv1+β1 = 55 ± 14; cbv1+β2-IR = 40 ± 3.3; cbv1+β3 = 80 ± 17; cbv1+β4 = 130 ± 8. τ_{deact} was estimated from tail currents after stepping down to −80 mV from V_{max}. *n* = 4–8; *, different from cbv1 ($P < 0.05$); #, different from cbv1+β1 ($P < 0.05$). Data are expressed as mean ± SEM.

β3 (variant d) with cbv1 was characterized by lack of modulation of cbv1's apparent Ca^{2+}_i sensitivity, activation, or deactivation kinetics. At 10 µM, τ_{act} and τ_{deact} values were 1.40 ± 0.10 and 1.13 ± 0.13 ms versus 1.91 ± 0.73 and 0.76 ± 0.11 ms for cbv1 versus cbv1+β3, respectively (Fig. 1, A–D). These data are in agreement with previous studies on slo1±β3 other than cbv1 (Behrens et al., 2000; Brenner et al., 2000a; Uebele et al., 2000; Zeng et al., 2008). Membrane surface coexpression of β3d subunit with cbv1 was confirmed by conducting biotinylation followed by Western blotting (Fig. S1 A). In addition, β3d coexpression resulted in longer channel openings (Fig. S1 B), as previously reported (Bukiya et al., 2013). In contrast to β1- and β2-IR–induced modifications in ionic current phenotype, expression of β4 increased cbv1 $V_{0.5}$ at 0.3–10 µM Ca^{2+}_i while decreasing $V_{0.5}$ at 30–100 µM Ca^{2+}_i (Fig. 1 B). In addition, at 10 µM Ca^{2+}_i, β4 significantly increased τ_{act} from its cbv1 value, 1.40 ± 0.1 ms to 4.25 ± 0.83 ms ($P < 0.05$), while increasing τ_{deact} from its cbv1 value ($P < 0.05$; Fig. 1, C and D). Thus, the β4-introduced changes in $V_{0.5}$, τ_{act}, and τ_{deact} over cbv1's values are consistent with those previously reported for β4 and slo1 channels other than cbv1 (Behrens et al., 2000; Brenner et al., 2000a; Orio et al., 2002). Collectively, results from this section established that BK channel complexes that result from expressing the same slo1 (cbv1) subunit when each type of BK β subunit known so far renders macroscopic current phenotypes that are similar to those reported with matching β subunits and different *Slo1* gene products. These similarities in $V_{0.5}$, τ_{act}, and τ_{deact} together with our previous pharmacological data obtained with cbv1±β subunits that matched published studies on slo1+β subunits other

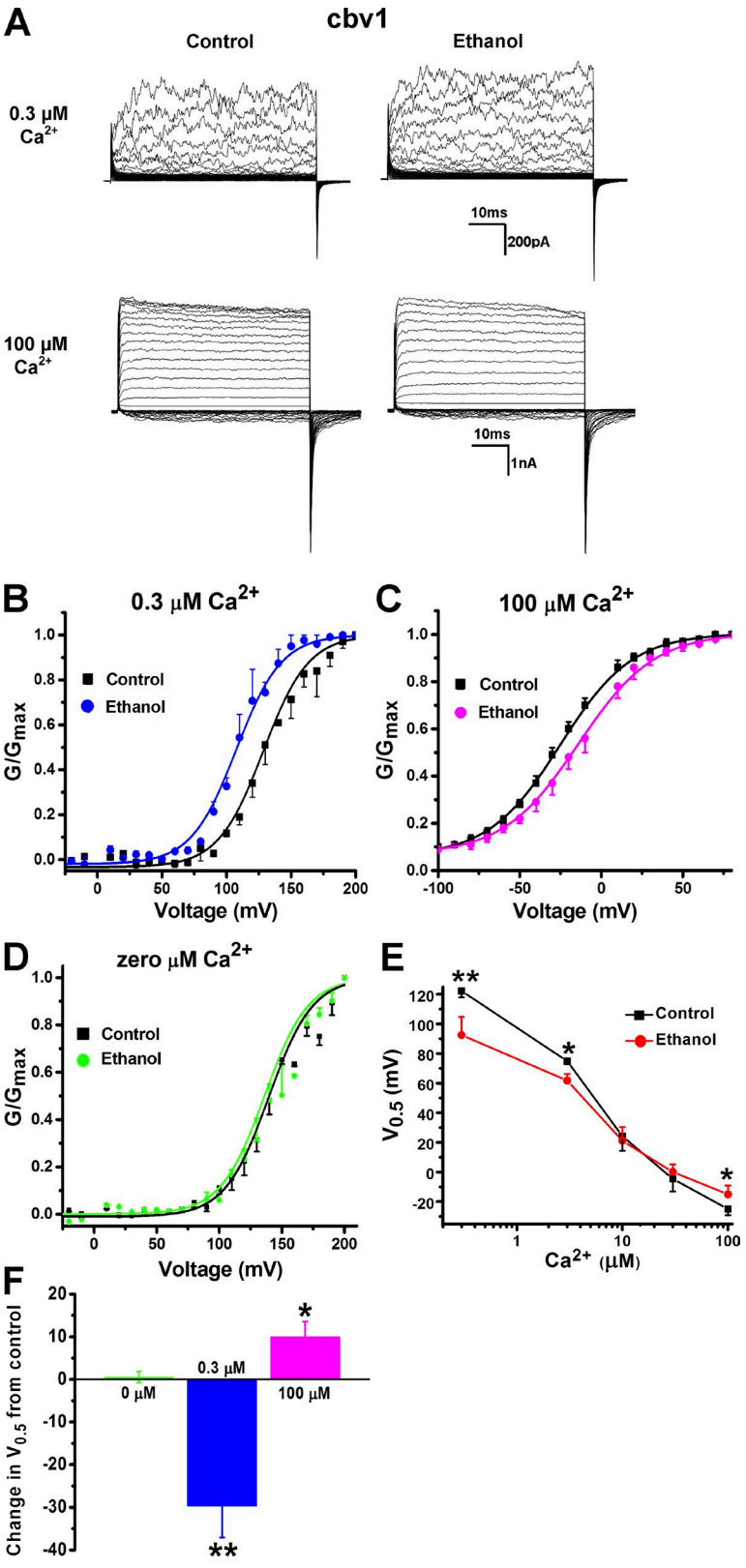

Figure 2. **Ethanol effect on BK macroscopic currents is Ca^{2+}_i dependent.** 50 mM ethanol activates homomeric cbv1 channels at submicromolar (0.3 μM) Ca^{2+}_i while causing mild inhibition at higher Ca^{2+}_i (100 μM). (A) Macroscopic current recordings evoked from I/O patches at 0.3 and 100 μM Ca^{2+}_i in the absence or presence of 50 mM ethanol after cbv1 expression in *Xenopus* oocytes. (B) At 0.3 μM Ca^{2+}_i, ethanol shifts the G/G_{max}-V plot to the left, indicating channel activation. (C) At 100 μM Ca^{2+}_i, ethanol shifts the G/G_{max}-V plot to the right, indicating inhibition of channel activity. (D) At nominal zero Ca^{2+}_i, ethanol does not shift the G/G_{max}-V plot, indicating ethanol fails to modulate cbv1 channel activity at nominal zero Ca^{2+}_i. (E) $V_{0.5}$ versus $[Ca^{2+}]_i$ plot showing that the activation to inhibition crossover for ethanol effect on cbv1 currents occurs at ≈20 μM Ca^{2+}_i. (F) Bar graph showing ethanol-induced change in $V_{0.5}$ from control obtained at nominal zero, 0.3, and 100 μM Ca^{2+}_i. *n* = 5–8; each patch was excised from a different cell. *, different from control ($P < 0.05$); **, different from control ($P < 0.01$). Data are expressed as mean ± SEM.

than cbv1 (Bukiya et al., 2007, 2009b, 2013; Kuntamallappanavar et al., 2014) underscore the major role of BK auxiliary β proteins in determining the final BK ionic current phenotype and its pharmacology.

Ethanol direct modulation of homomeric cbv1-mediated current is Ca^{2+}_i dependent but not Mg^{2+}_i dependent

First, we evaluated ethanol direct action (i.e., independently of cytosolic signaling or alcohol metabolism)

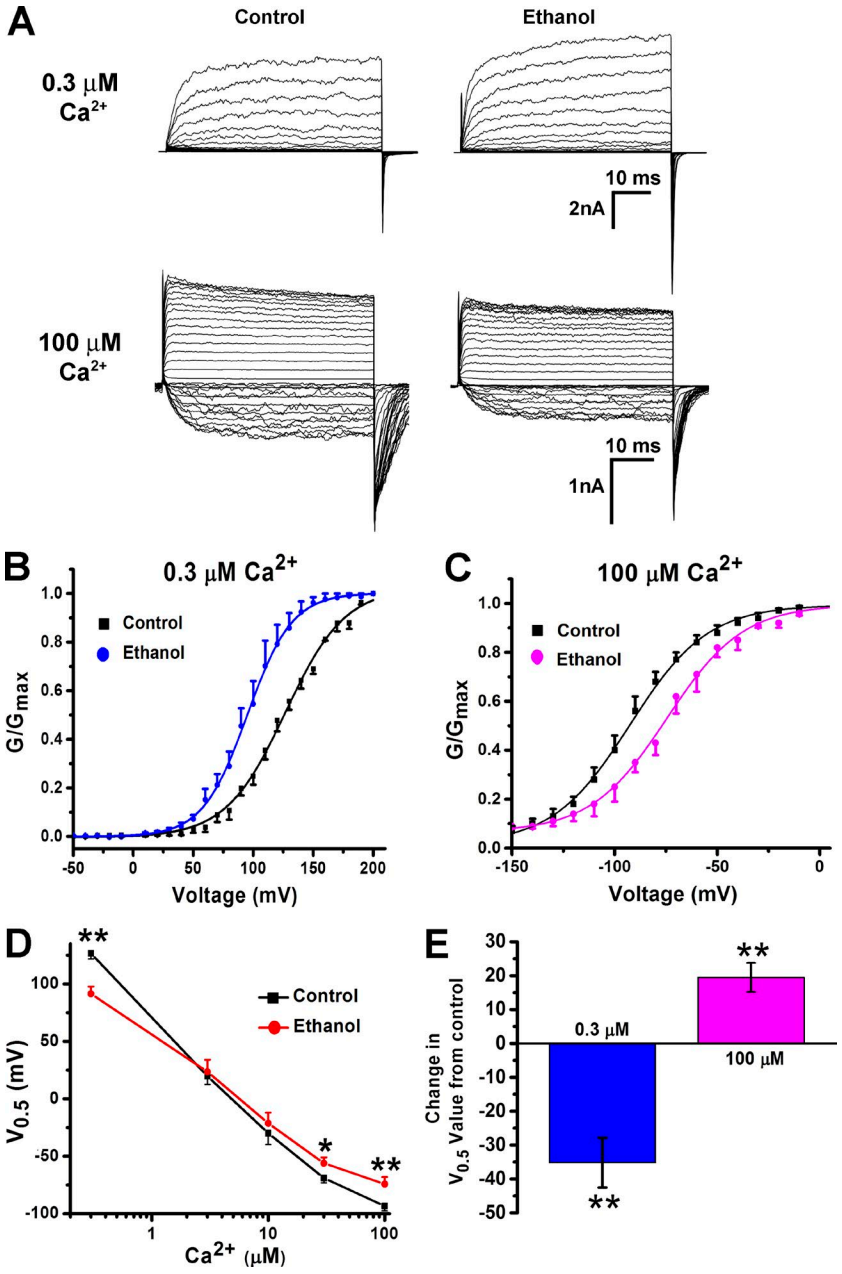

Figure 3. **Ethanol activates β1-containing BK channels at submicromolar (0.3 μM) Ca^{2+}_i, while causing strong inhibition at higher (100 μM) Ca^{2+}_i.** (A) Macroscopic current recordings from I/O patches obtained at 0.3 and 100 μM Ca^{2+}_i in the absence or presence of 50 mM ethanol after cbv1+β1 expression in *Xenopus* oocytes. (B and C) Ethanol shifts the G/G_{max}-V plot to the left at 0.3 μM Ca^{2+}_i, indicating BK current potentiation (B), while shifting the plot to the right at 100 μM Ca^{2+}_i, indicating inhibition (C). (D) β1 subunits set the activation to inhibition crossover of ethanol responses at ≈3 μM Ca^{2+}_i. (E) Bar graph representing ethanol-induced change in $V_{0.5}$ values from pre-ethanol application obtained at 0.3 μM and 100 μM Ca^{2+}_i. *n* = 5–8; each patch was excised from a different cell. *, different from control ($P < 0.05$); **, different from control ($P < 0.01$). Data are expressed as mean ± SEM.

on homomeric cbv1 channels using excised, cell-free patches under continuous perfusion with divalent-buffered solutions. Thus, macroscopic currents were obtained over a wide range of activating Ca^{2+}_i (0–100 μM) in the presence and absence of 50 mM ethanol. Ethanol increased cbv1 channel activity at low $[Ca^{2+}]_i$ i.e., 0.3–10 μM, which was evident as a shift to the left in the G/G_{max}-V plot and eventual decrease in $V_{0.5}$ as shown in the $V_{0.5}$-$[Ca^{2+}]_i$ plot (Fig. 2, A, B, E, and F). However, ethanol did not modulate cbv1 channel activity at zero Ca^{2+}_i (Fig. 2, D and F). Moreover, as $[Ca^{2+}]_i$ increased (30–100 μM), ethanol-induced channel activation turned to inhibition, which was evident as a small right shift in the G/G_{max}-V plot and, eventually, a small increase in $V_{0.5}$ ($P < 0.05$; Fig. 2, C and E). Thus, ethanol-induced activation to inhibition crossover occurred at ∼20 μM (Fig. 2 E). These results demonstrate that ethanol action on cbv1 channels not only depends on Ca^{2+}_i presence but is also a function of $[Ca^{2+}]_i$. This result extends previous findings with slo1 channels cloned from mouse brain (mslo1, mbr5 variant) and heterologously expressed in the same expression system (Liu et al., 2008).

Previous studies have clearly established that BK channels can be gated by millimolar levels of Mg^{2+}_i, independently of Ca^{2+}_i-driven gating (Shi et al., 2002). Thus, we next obtained macroscopic current recordings from Mg^{2+}_i-gated cbv1 channels over a wide range of activating $[Mg^{2+}]_i$ (0–100 mM) in the presence and absence of 50 mM ethanol (Fig. S2 A). Remarkably, ethanol failed to modulate cbv1-mediated current across

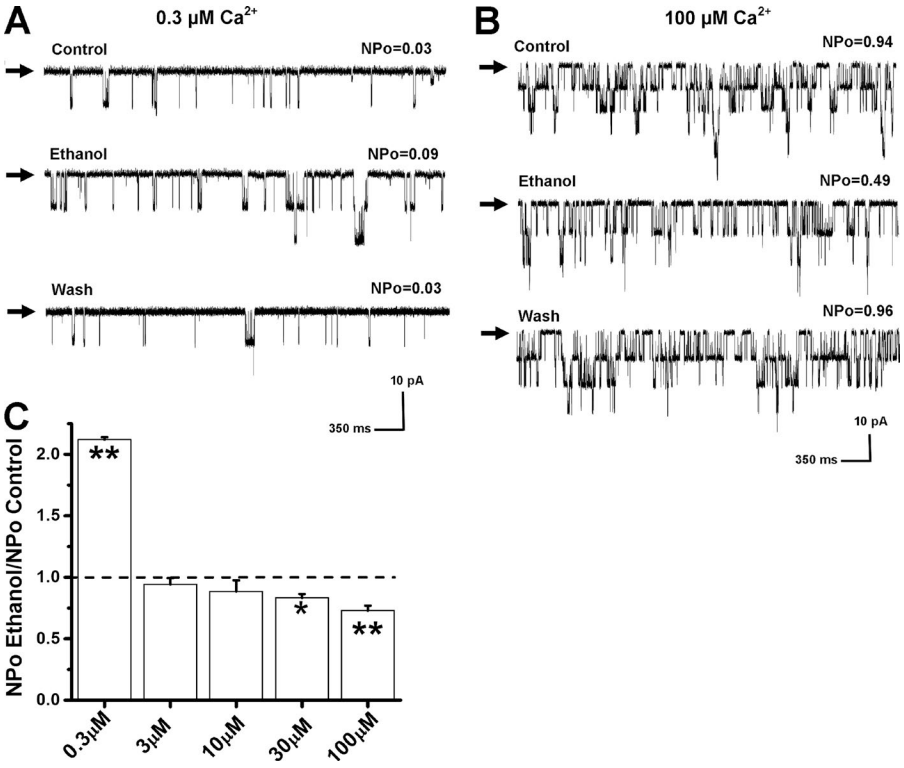

Figure 4. **The ethanol response of wt β2–containing BK channels is similar to the ethanol response of cbv1+β1 channels.** (A and B) Single-channel recordings of cbv1+wt β2 channels from I/O patches at 0.3 (A) and 100 μM Ca^{2+}_i (B); V_m = −40 mV. Records were obtained before (top traces), during (middle traces), and immediately after (bottom traces) patch exposure to 50 mM ethanol. Arrows indicate the baseline (all channels in nonpermeant states). (C) Averaged NPo ratios in the presence and absence of ethanol from cbv1+wt β2 at 0.3, 3, 10, 30, and 100 μM Ca^{2+}_i. Data demonstrate that the activation to inhibition crossover for ethanol effect on cbv1+wt β2 channels occurs at ≈3 μM Ca^{2+}_i, which is similar to that found in cbv1+β1 channels. *n* = 5–7; each patch was excised from a different cell. *, different from control (P < 0.05); **, different from control (P < 0.01). Data are expressed as mean ± SEM.

all Mg^{2+}_i levels, which was evident from the lack of significant differences in G/G_{max}-V and $V_{0.5}$-$[Mg^{2+}]$ plots between control and ethanol-containing solutions (Fig. S2, B–D). These findings demonstrate that, when cbv1 channels are gated by Mg^{2+}_i, their sensitivity to high, intoxicating levels of ethanol (50 mM) is lost. The result underscores the specificity of Ca^{2+}_i over other ions in determining the sensitivity of BK channel gating to ethanol (Liu et al., 2013).

BK β1 subunit facilitates ethanol-induced inhibition of β1-containing BK channel complexes

After demonstrating that β1 and ethanol modulation of cbv1 current were both Ca^{2+}_i dependent (Figs. 1 B and 2 E), we next addressed the functional interactions between β1 and ethanol that resulted in regulating the cbv1 channel function. 50 mM ethanol activated cbv1+β1 channels at low $[Ca^{2+}]_i$, i.e., 0.3 μM, which was evident as a leftward shift in the G/G_{max}-V plot (Fig. 3, A and B) and thus a decrease in $V_{0.5}$ value in the $V_{0.5}$-$[Ca^{2+}_i]$ plot (P < 0.01; Fig. 3, D and E). As $[Ca^{2+}]_i$ increased (3–100 μM), activation turned to increasingly significant inhibition (P < 0.05 at 30 μM and P < 0.01 at 100 μM), which was evident as a rightward shift in the G/G_{max}-V plot (Fig. 3 C) and eventual increase in $V_{0.5}$ values, as seen in the $V_{0.5}$-$[Ca^{2+}]_i$ plot (Fig. 3, D and E). Furthermore, ethanol-induced activation to inhibition crossover shifted to ∼3 μM (Fig. 3 D) from that of cbv1 channels (∼20 μM), that is, almost one log unit decrease. Our data demonstrate that ethanol-mediated inhibition of recombinant BK channels made of subunits (cbv1+β1) cloned from rat cerebral artery myocytes occurs at physiological Ca^{2+}_i (4–30 μM) and voltage (−60 to −20 mV) found near native BK channels during contraction of rat cerebral artery myocytes (Pérez et al., 2001).

Ethanol responses of wt β2- and β2-IR–containing BK channel activity are similar to that of β1 subunit–containing BK channels

After characterizing the effect of ethanol on the Ca^{2+}_i dependence of macroscopic current from cbv1+β1 versus cbv1 channels (previous paragraph) and having demonstrated that the Ca^{2+}_i dependence of macroscopic current was similarly modified when cbv1 channels were coexpressed with β1 or β2-IR subunits (Fig. 1 B), we next determined whether β1-induced modification of ethanol action on the $V_{0.5}$-$[Ca^{2+}]_i$ plot of cbv1 channels was unique to this subunit or, rather, matched by coexpression of wt β2 or β2-IR with cbv1. Coexpression of wt β2 with cbv1 evoked rapidly inactivating macroscopic currents, as initially shown in Fig. 1 A. Then, we evaluated ionic currents at single-channel resolution obtained from I/O patches in gap-free recordings at V_m = −20 to −40 mV and over a wide range of Ca^{2+}_i for 30 s under each experimental condition (control vs. 50 mM ethanol). Ethanol activated cbv1+wt β2 channels at low $[Ca^{2+}]_i$, i.e., 0.3 μM, which was evident as a robust increase in NPo (P < 0.01; Fig. 4, A and C). As $[Ca^{2+}]_i$ increased, this activation turned into inhibition, which was evident as a significant reduction in NPo (P < 0.01; Fig. 4, B and C). Furthermore, as

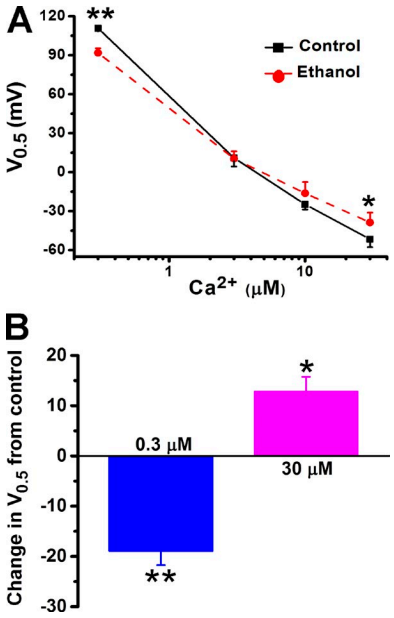

Figure 5. **The ethanol response of β2-IR–containing BK channels is similar to the ethanol response of cbv1+β1 channels.** (A) $V_{0.5}$ versus $[Ca^{2+}]_i$ plot showing that the activation to inhibition crossover for ethanol effect on cbv1+β2-IR channels occurs at ≈3 μM Ca^{2+}_i, as found with cbv1±β1 (Fig. 3 D) and wt β2 (Fig. 4 C). (B) Bar graph showing ethanol-induced change in $V_{0.5}$ values from control obtained at 0.3 and 100 μM Ca^{2+}_i. *n* = 4–6 patches; each patch was excised from a different cell. *, different from control ($P < 0.05$); **, different from control ($P < 0.01$). Data are expressed as mean ± SEM.

found with cbv1+β1 (Fig. 3 D), ethanol-induced activation to inhibition crossover of cbv1+wt β2 occurred at ∼3 μM (Fig. 4 C). These experiments of ethanol action on cbv1+wt β2 complexes at single-channel resolution were matched by experiments using macroscopic recordings (Fig. S3). Likewise, ethanol activated cbv1+β2-IR channels at low $[Ca^{2+}]_i$, i.e., 0.3 μM, which was evident as a marked decrease in $V_{0.5}$ values in the $V_{0.5}$-$[Ca^{2+}]_i$ plot ($P < 0.01$; Fig. 5, A and B). As $[Ca^{2+}]_i$ increased, ethanol-induced potentiation of ionic current turned to inhibition, which was evident as a significant ($P < 0.05$) increase in $V_{0.5}$ values in the $V_{0.5}$-$[Ca^{2+}]_i$ plot (Fig. 5, A and B). As previously found with cbv1+β1 and cbv1+wt β2, ethanol-induced activation to inhibition crossover of cbv1+β2-IR currents occurred at ∼3 μM (Fig. 5 A). The similarity of ethanol action on cbv1+wt β2 versus cbv1+β2-IR strongly suggests that the inactivation domain of wt β2 does not play a significant role in ethanol action on these channels. However, the similarity of ethanol's overall effect among cbv1+β1, cbv1+wt β2, and cbv1+β2-IR constructs raises the speculation that ethanol action on heteromeric BK channels is somewhat linked to channel gating processes commonly affected by these regulatory subunits, very likely gating transitions that contribute to determine the apparent Ca^{2+}_i sensitivity of the channel complex.

Ethanol responses of β3- and β4-containing BK currents are similar to that of currents evoked by homomeric cbv1 channels

When compared with β1 and β2-IR subunits, β3 and β4 subunits have a milder effect on the apparent Ca^{2+}_i sensitivity of slo1 channels, as documented by several groups, including our laboratory (Fig. 1 B; Xia et al., 1999; Behrens et al., 2000; Brenner et al., 2000a; Uebele et al., 2000; Bao and Cox, 2005; Orio and Latorre, 2005; Bukiya et al., 2009a,b, 2013; Sun et al., 2013; Kuntamallappanavar et al., 2014). If the hypothesis raised at the end of the previous section is true, ethanol action on β3- or β4-containing BK channels should not greatly differ from ethanol action on homomeric cbv1. Thus, cbv1+β3 and cbv1+β4 were coexpressed and probed with 50 mM ethanol under experimental conditions similar to those of the cbv1±β1/wt β2/β2-IR experiments. Ethanol activated cbv1+β3 and cbv1+β4 channels at low $[Ca^{2+}]_i$, i.e., 0.3 μM, which was evident as a marked decrease in $V_{0.5}$ from the $V_{0.5}$-$[Ca^{2+}]_i$ plot ($P < 0.01$; Fig. 6, A–D). As $[Ca^{2+}]_i$ increased, this activation turned into mild inhibition, which could be noticed by a significant increase ($P < 0.05$) in $V_{0.5}$ from the $V_{0.5}$-$[Ca^{2+}]_i$ plot (Fig. 6, A–D). In both heteromeric BK complexes, ethanol-induced activation to inhibition crossover occurred at ∼20 μM (Fig. 6, A and C). Thus, β3- and β4-containing BK channel responses to ethanol did match that of homomeric cbv1 channels, indicating that β3 and β4 subunits do not noticeably modulate ethanol action on ionic currents mediated by homomeric cbv1 channels.

Ca^{2+}_i-independent gating processes of homomeric BK channels remain unaffected by ethanol

Once we established that (a) ethanol differentially modulated BK channels containing different β subunit compositions, having identified two basic phenotypes: (1) ethanol action on homomeric cbv1 (matched by cbv1+β3 or cbv1+β4 complexes) and (2) ethanol action on cbv1+β1 (matched by cbv1+wt β2/β2-IR), and (b) ethanol direct action on macroscopic current depended on Ca^{2+}_i presence and was modulated by this divalent, yet not by Mg^{2+}_i, we decided to address which specific BK channel gating mechanisms could explain ethanol action, with a focus on selective allosteric coupling between ethanol and Ca^{2+}_i. Thus, we evaluated ethanol action on cbv1±β1 channels under a wide variety of experimental conditions to fit experimental data to the 70-state HA allosteric gating model (Horrigan and Aldrich, 1999, 2002; Horrigan et al., 1999; Orio and Latorre, 2005).

It has been previously demonstrated that, by obtaining the Po-V relationship of BK channels at very negative potentials and nominal zero Ca^{2+}_i, it is possible to directly estimate two parameters associated with the channel's closed to open conformational change (or intrinsic gating), i.e., L_0 and z_L, which indicate closed to

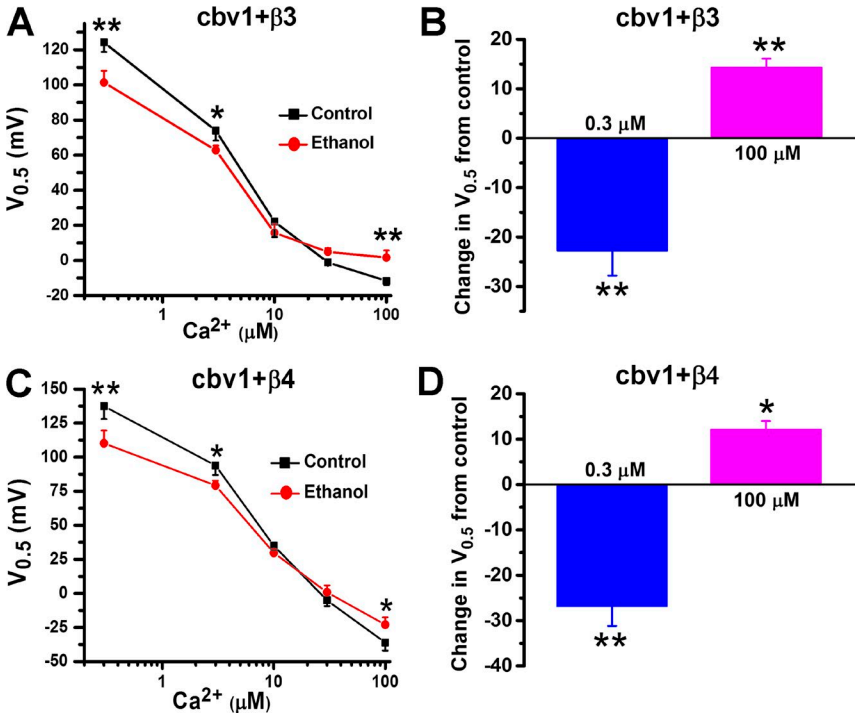

Figure 6. **Ethanol responses of β3- or β4-containing BK currents mimic those of homomeric BK (cbv1) channels.** (A and C) $V_{0.5}$ versus $[Ca^{2+}]_i$ plot showing that the activation to inhibition crossover for ethanol effect on cbv1+β3 (A) and cbv1+β4 channel complexes (C) occurs at ~20 μM Ca^{2+}_i, as found for homomeric cbv1 exposed to ethanol (see Fig. 2 D). (B and D) Bar graphs representing ethanol-induced change in $V_{0.5}$ values from cbv1+β3 (B) and cbv1+β4 channel complexes (D) obtained at 0.3 μM and 100 μM Ca^{2+}_i. *n* = 3–7 patches; each patch was excised from a different cell. *, different from control ($P < 0.05$); **, different from control ($P < 0.01$). Data are expressed as mean ± SEM.

open equilibrium constant at V = 0 when no Ca^{2+}_i is bound to the channel and gating charge associated with channel opening, respectively (Horrigan and Aldrich, 1999, 2002; Horrigan et al., 1999). For cbv1 channels (Fig. 7 A), the best-fit values were $L_0 = 2.3 \times 10^{-6} \pm 6.3 \times 10^{-7}$ and $z_L = 0.34 \pm 0.054$ (Fig. 7 B), matching previously published data from slo1 channels other than cbv1 (Horrigan and Aldrich, 1999, 2002; Bao and Cox, 2005; Orio and Latorre, 2005; Sun et al., 2013). Ethanol, however, failed to alter these parameters, $L_0 = 2.1 \times 10^{-6} \pm 2.8 \times 10^{-7}$ and $z_L = 0.35 \pm 0.04$ both in the presence of 50 mM ethanol (Fig. 7, B and C), indicating that ethanol at concentrations that increase BK Po does not modulate the conformational change associated with the closed to open transition of the channel.

After establishing that ethanol did not modify cbv1 L_0 or z_L, we next evaluated ethanol action on parameters $V_h(J)$, z_J, and D, which indicate half-activation voltage of voltage sensors when the channel is closed, gating charge associated with voltage sensor movement, and allosteric interaction of voltage sensor activation with channel opening, respectively. To perform this, we combined Po-V data with G/G_{max}-V data to obtain channel activity–V curves across the necessarily wide voltage range (Fig. 8, A and B). The resulting curves were fitted with Eq. 3. While fitting the data obtained from cbv1 channels in the absence of ethanol, $V_h(J)$, L_0, and z_L were constrained to 155 (Horrigan et al., 1999), 2.3×10^{-6}, and 0.34 (see Fig. 7), respectively, whereas D and z_J were allowed to vary. For ethanol data, L_0 and z_L values were constrained to 2.1×10^{-6} and 0.35, respectively, whereas $V_h(J)$, D, and z_J were allowed to vary. In the absence of ethanol, fitting results rendered D = 19.8 ± 1.4 and $z_J = 0.61 \pm 0.05$ for cbv1 channels (Fig. 8 A). These results are quite similar to the values obtained by different groups using slo1 channels other than cbv1 (Horrigan and Aldrich, 1999, 2002; Cox and Aldrich, 2000; Bao and Cox, 2005; Orio and Latorre, 2005).

$V_h(J)$, D, and z_J from cbv1 channels remained unmodified by 50 mM ethanol: $V_h(J) = 154.1 \pm 2.7$, D = 19.6 ± 0.6, and $z_J = 0.6 \pm 0.05$ (Fig. 8 B). These data indicate that ethanol at concentrations obtained during binge drinking, while altering BK channel steady-state activity in the presence of Ca^{2+} (Dopico et al., 1998; Liu et al., 2008), does not alter the movement of voltage sensors when the channel is closed, the gating charge associated with the voltage sensor movement, or the coupling factor between voltage sensor activation and channel opening. Collectively, all the ethanol data shown so far indicate that, at physiological Ca^{2+}_i levels, ethanol markedly increases cbv1 channel activity without significantly modifying any of the Ca^{2+}_i-independent gating processes under study.

Ethanol enhances the apparent Ca^{2+}_i binding affinity of homomeric BK channels

Next, we addressed ethanol action on major Ca^{2+}_i-dependent gating processes of homomeric cbv1 channels. Several studies have demonstrated that two Ca^{2+}_i-dependent gating parameters (i.e., K_d and C, Ca^{2+} binding affinity and allosteric factor coupling Ca^{2+}_i binding with channel opening, respectively) can be estimated from the Ca^{2+} dependence of Po at very negative voltages (Horrigan and Aldrich, 1999, 2002; Horrigan et al.,

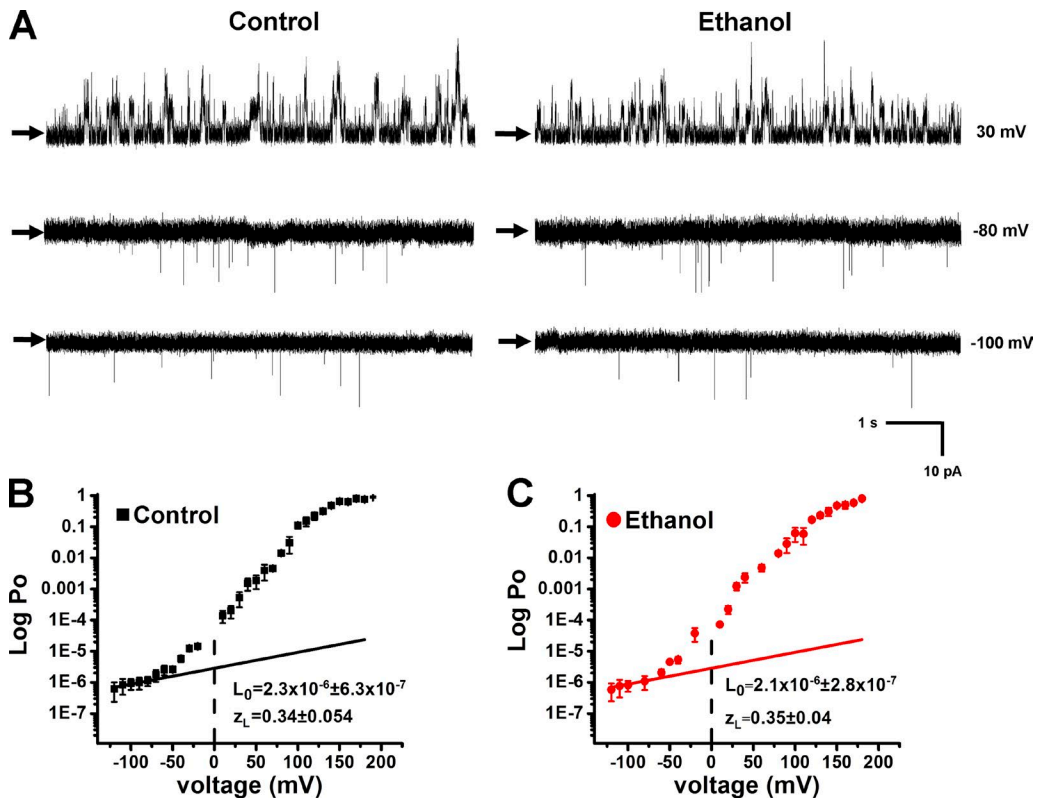

Figure 7. **Ethanol does not alter the parameters associated with closed to open conformational change.** (A) Representative unitary current recordings evoked from I/O patches in nominal zero Ca^{2+}_i, with membrane patches held at the indicated voltages. Recordings were obtained before (left) and immediately after (right) patch exposure to 50 mM ethanol. Arrows indicate the baseline (all channels in nonpermeant states). (B and C) Mean log Po-V relations over a wide range of voltages in the presence and absence of 50 mM ethanol. Below 80 mV, data points were obtained from unitary current recordings; above 80 mV, data points were obtained from macroscopic current recordings in nominal zero Ca^{2+}_i. Po-V data at far negative voltages were fitted with Eq. 2 to determine L_0 and z_L. Best-fit parameters (±95% confidence interval) are listed in the corresponding graphs. On average, patches contained 450 channels. *n* = 11; each patch was excised from a different cell. Data are expressed as mean ± SEM.

1999; Sweet and Cox, 2008, 2009). Thus, we obtained R_0 (i.e., the NPo ratio in the presence and absence of Ca^{2+}_i; see Materials and methods) at very negative voltages (−80 mV) in the absence and presence of 50 mM ethanol, and data were fitted with Eq. 5. Best-fit values were K_d = 9.02 ± 1.4 and C = 6.07 ± 0.1, matching previously published data for slo1 channels other than cbv1 (Horrigan and Aldrich, 1999, 2002; Bao and Cox, 2005; Orio and Latorre, 2005; Sun et al., 2013). Remarkably, ethanol decreased K_d from 9.02 ± 1.4 to 1 ± 0.07 (~90% decrease). In contrast, ethanol decreased C from 6.07 ± 0.1 to 4.7 ± 0.12 (~20% decrease; Fig. 9, A and B). Therefore, ethanol-induced potentiation of cbv1 current is basically the result of a nine-times increase in the channel's apparent Ca^{2+} binding affinity, in spite of an ~20% reduction in the efficacy of coupling between Ca^{2+} binding and channel opening.

Next, we examined ethanol action on parameter E, which indicates the allosteric interaction of Ca^{2+} binding with voltage sensor activation. Estimation of the

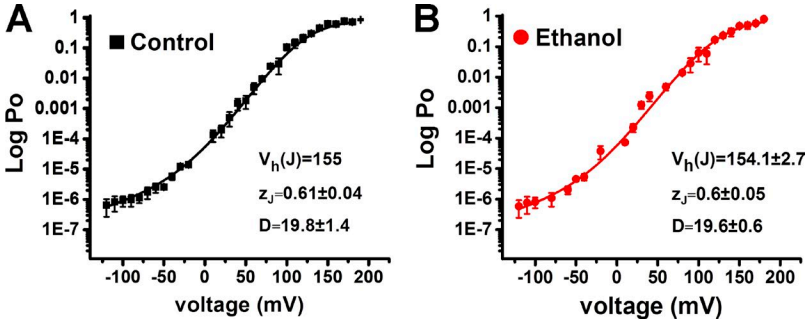

Figure 8. **Ethanol does not alter movement of voltage sensors and other voltage-dependent parameters of cbv1 channels.** (A and B) Po-V data over a wide range of voltages were fitted with Eq. 3 after constraining V_h(J), L_0, and z_L (Fig. 7; Horrigan and Aldrich, 2002) to determine the values of D and z_J. For ethanol data, V_h(J) was allowed to vary. Best-fit parameters (±95% confidence interval) are listed in the corresponding graphs. *n* = 11; each patch was excised from a different cell. Data are expressed as mean ± SEM.

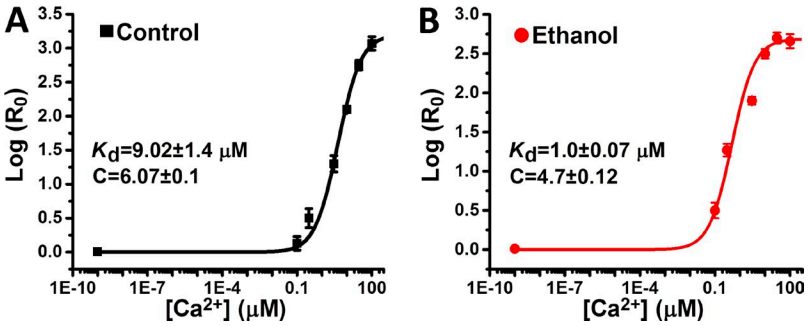

Figure 9. **Ethanol modulates parameters associated with Ca^{2+}_i binding to cbv1 channels.** (A and B) The averaged (log $[R_0]$)-$[Ca^{2+}_i]$ plots (voltage: −80 mV) in the absence (A) and presence (B) of 50 mM ethanol. (log $[R_0]$)-Ca^{2+}_i plots were fitted with the Eq. 5. Best-fit parameters (±95% confidence interval) are shown to the left of the corresponding plots. Data demonstrate that ethanol action on cbv1 is primarily caused by modulation of K_d and C. n = 4; each patch was excised from a different cell. Data are expressed as mean ± SEM.

value E from ionic current measurement alone is somewhat difficult. To determine E, however, we obtained G/G_{max}-V relationships at various Ca^{2+}_i concentrations from nominal zero to 100 μM in the presence and absence of 50 mM ethanol and fitted the curves to Eq. 1 by minimizing least-squares with a mixture of Marquardt–Levenberg and Simplex iterations (Orio and Latorre, 2005). $V_h(J)$, L_0, z_L, z_J, D, K_d, and C were constrained to the following values for control versus ethanol data (as previously determined from data shown in Figs. 7, 8, and 9): $V_h(J)$ = 155 mV versus 154.1 mV; $L_0 = 2.3 \times 10^{-6}$ versus 2.1×10^{-6}; z_L = 0.34 versus 0.35; K_d = 9.02 versus 1; and C = 6.07 versus 4.7, whereas E was allowed to vary. Several fits were conducted with different sets of initial parameters, and the fits with lower χ^2 values were chosen. Best-fit results for cbv1 in the absence of ethanol rendered E = 6.15 ± 2.1 (Fig. 10 A), which is in reasonable agreement with previously obtained best-fit values for slo1 channels other than cbv1 (Horrigan and Aldrich, 1999, 2002; Orio and Latorre, 2005). Ethanol, however, did not alter E (Fig. 10, A and B), underscoring that the alcohol does not modify the allosteric interaction between Ca^{2+} binding and voltage sensor activation of homomeric cbv1 channels. Collectively, our results indicate that most of ethanol's effect on homomeric BK (cbv1) channels is caused by modifying drug-induced increase in Ca^{2+}_i binding affinity and allosteric interaction between Ca^{2+}_i binding and channel opening, thereby modulating overall channel activity.

In the presence of β1 subunits, Ca^{2+}_i-independent gating processes of BK channels remain unaffected by ethanol

In contrast to cbv1 data, log (Po)-V plots from cbv1+β1 channels did not reach the limiting slope (Fig. 11, A and B), as reported by several groups using slo1 other than cbv1 (Bao and Cox, 2005; Orio and Latorre, 2005; Sun et al., 2013). Therefore, for cbv1+β1 channels, we determined the effect of ethanol on voltage sensor movement ($V_h(J)$), parameters associated with closed to open conformation change (L_0 and z_L), and voltage dependence of gating (z_J and D) by fitting the Po-V data with Eq. 3 (Fig. 11, A and B). For control data, $V_h(J)$ was constrained to a previously published value, i.e., 80 mV (Bao and Cox, 2005), whereas L_0, z_L, D, and z_J were allowed to vary freely. Our fitting results obtained for cbv1+β1 channels in the absence of ethanol resulted in $L_0 = 1.2 \times 10^{-7} \pm 4.4 \times 10^{-8}$, z_L = 0.41 ± 0.06, D = 30.2 ± 3.7, and z_J = 0.6 ± 0.03 (Fig. 11 B). These values reasonably match the values obtained by different groups for slo1 other than cbv1 when coexpressed with β1 (Cox and Aldrich, 2000; Orio and Latorre, 2005; Sun et al., 2013). As found for cbv1 channels, ethanol failed to modify any of these parameters: $V_h(J)$ = 80.8 ± 1.6, $L_0 = 1.3 \times 10^{-7} \pm 3.9 \times 10^{-8}$, z_L = 0.42 ± 0.3, D = 29.3 ± 2.6, and

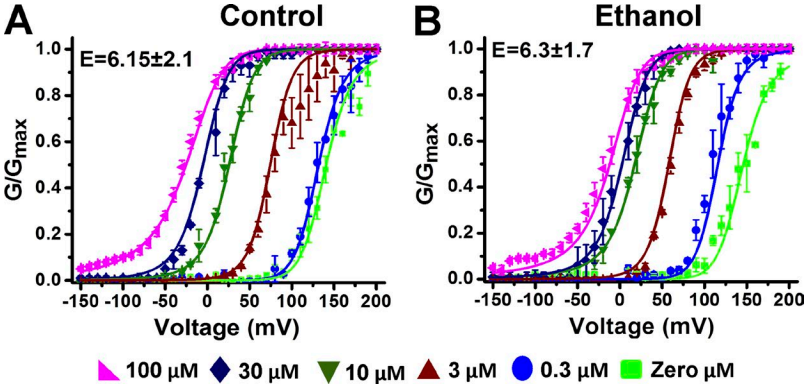

Figure 10. **Ethanol does not alter the allosteric interaction between Ca^{2+} binding and voltage sensor activation of cbv1 channels.** (A and B) Averaged G/G_{max}-V curves obtained over a wide range of Ca^{2+}_i in the absence (A) and presence (B) of 50 mM ethanol. G/G_{max}-V plots were fitted with Eq. 1. For curves in panel A, L_0, z_L, $V_h(J)$, z_J, D, K_d, and C were constrained to 2.3×10^{-6}, 0.34, 155, 0.6, 19.8, 9.02, and 6.07, respectively (Figs. 7, 8, and 9), whereas E was allowed to vary. For G-V curves in panel B, L_0, z_L, $V_h(J)$, z_J, D, K_d, and C were fixed to 2.1×10^{-6}, 0.35, 155.1, 0.6, 19.6, 1, and 4.7, respectively, whereas E was allowed to vary. Best-fit parameters (±95% confidence interval) are shown to the left of the corresponding plots. n = 4–8; each patch was excised from a different cell. Data are expressed as mean ± SEM.

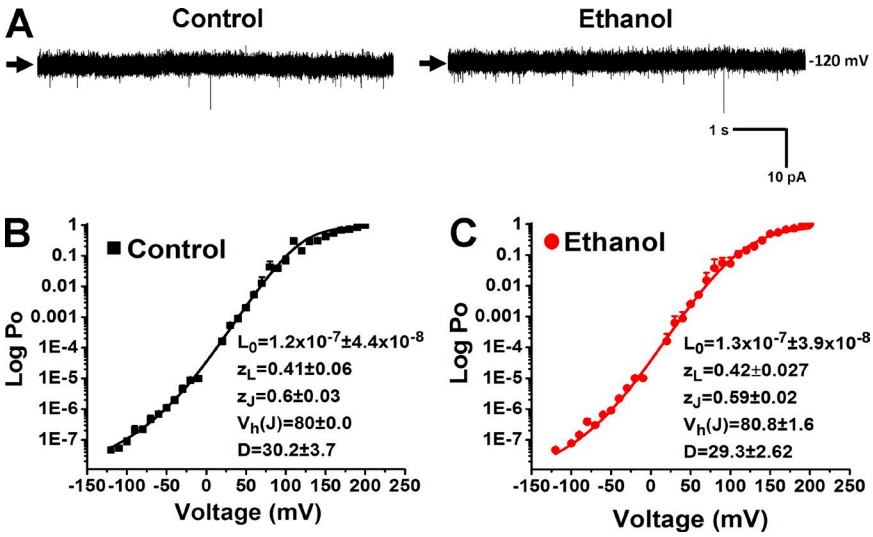

Figure 11. **Ethanol does not alter the voltage-dependent parameters of cbv1+β1 channels.** (A–C) Representative current traces (A) and mean log Po-V relations in the absence (B) and presence (C) of 50 mM ethanol. At voltages less positive than 80 mV, data points were obtained from unitary current recordings; at voltages more positive than 80 mV, data points were obtained from macroscopic current recordings obtained at nominal zero Ca^{2+}_i. Po-V data obtained over a wide range of voltages were fitted with Eq. 2 to determine the values of V_h(J), L_0, z_L, D, and z_J. For control data, V_h(J) was constrained to 80 mV (according to Bao and Cox [2005]), whereas for ethanol data V_h(J) was allowed to vary. Best-fit parameters (±95% confidence interval) are listed in the corresponding graphs. *n* = 12; each patch was excised from a different cell. Data are expressed as mean ± SEM.

z_J = 0.59 ± 0.02 in the presence of 50 mM ethanol (Fig. 11 B). In summary, when cbv1+β1 channels are probed with ethanol, the drug does not alter (a) the equilibrium constant between closed to open conformation, (b) the gating charge associated with such equilibrium constant, (c) the gating charge associated with the voltage sensor movement, or (d) the allosteric interaction between voltage sensor activation and channel opening. Collectively, these results indicate that ethanol, as found for homomeric cbv1 channels, does not modify the Ca^{2+}_i-independent gating processes of cbv1+β1 channels.

Ethanol modulates Ca^{2+}_i-dependent gating processes of β1-containing BK channels

To determine any possible effect of ethanol on the equilibrium governed by Ca^{2+}_i binding affinity (K_d) and its related allosteric factors (C and E), we used log (R_0)-V and G/G_{max}-V relations for cbv1+β1 channels in the presence and absence of ethanol at various Ca^{2+}_i concentrations from nominal zero to 100 µM. Then, log (R_0)-V relations were fitted with Eq. 5, and G/G_{max}-V relations were fitted with Eq. 1. Our best-fit values obtained for cbv1+β1 channels in the absence of ethanol were K_d = 19 ± 2.4, C = 27.2 ± 2.3 (Fig. 12 A), and E = 9.5 ± 1.6 (Fig. 13 A). As found for homomeric cbv1 channels, ethanol decreased K_d (from 19 ± 2.4 to 11.3 ± 1.2; Fig. 12 B). This decrease (~40%) in K_d corresponds to an approximately two-times increase in the apparent Ca^{2+} binding affinity, which is markedly smaller than the nine-times increase in Ca^{2+} binding affinity evoked by ethanol on homomeric channels (Fig. 9 and Tables 1 and 2). As found with homomeric cbv1 channels, ethanol decreased C (in this case from 27.2 ± 2.3 to 13.5 ± 0.45; Fig. 12 B). This decrease (~50%) in allosteric coupling between Ca^{2+} binding and channel opening is larger than the decrease evoked by the alcohol on homomeric channels (~20%). Finally, ethanol markedly decreased E by half: from 9.5 ± 1.6 to 4.06 ± 0.6 ($P < 0.05$; Fig. 13, A and B). It should be underscored that ethanol fails to modify this parameter when homomeric cbv1 channels are probed with the alcohol (Fig. 10 and Tables 1 and 2). Therefore, ethanol targets both common and distinct gating mechanisms in homomeric cbv1 versus cbv1+β1 channels, the former represented by K_d and C and the latter by E. Regarding the ethanol-sensitive common processes, a smaller increase in Ca^{2+} binding affinity and a larger decrease in allosteric interaction between Ca^{2+}_i binding and channel opening

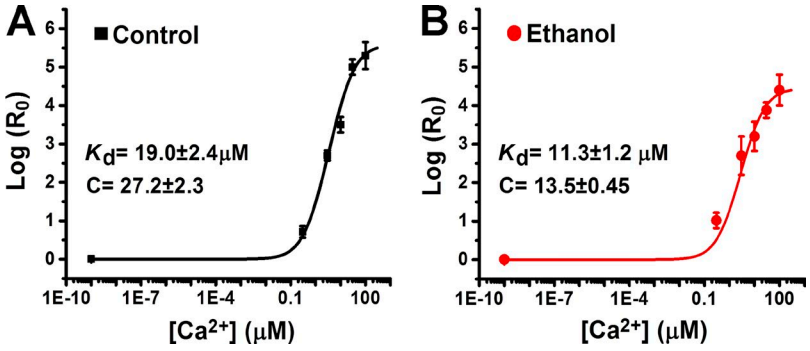

Figure 12. **Ethanol modulates parameters associated with Ca^{2+}_i binding affinity of cbv1+β1 channels.** (A and B) The averaged (log [R_0])-[Ca^{2+}_i] plots (voltage: −120 mV) in the absence (A) and presence (B) of 50 mM ethanol. (log [R_0])-[Ca^{2+}_i] plots were fitted with the Eq. 5. Best-fit parameters (±95% confidence interval) are shown to the left of the corresponding plots. Data demonstrate that ethanol significantly decreases the values of K_d and C. *n* = 4–5; each patch was excised from a different cell. Data are expressed as mean ± SEM.

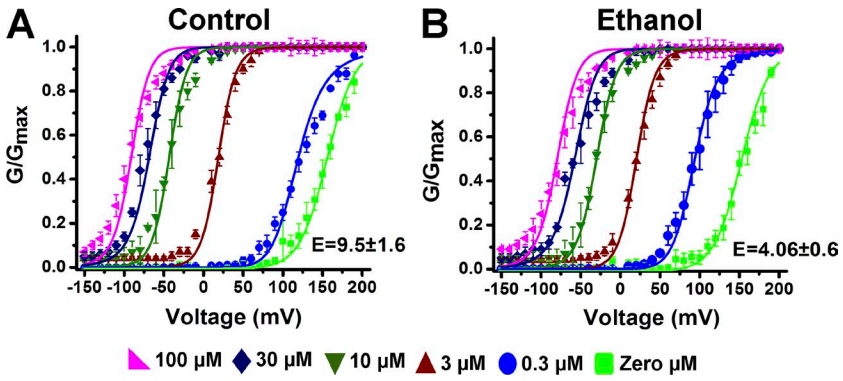

Figure 13. **Ethanol modulates allosteric interaction between Ca^{2+} binding and voltage sensor activation in cbv1+β1 channels.** (A and B) Averaged G/G_{max}-V curves obtained over a wide range of Ca^{2+}_i, in the absence (A) and presence (B) of 50 mM ethanol. These plots were fitted with Eq. 1. For curves in panel A, L_0, z_L, $V_h(J)$, z_J, D, K_d, and C were fixed to 1.25×10^{-7}, 0.41, 80, 0.6, 30.1, 19, and 27.2, respectively, whereas E was allowed to vary. For curves in panel B, L_0, z_L, $V_h(J)$, z_J, D, and K_d were fixed to 1.3×10^{-7}, 0.42, 80.83, 0.59, 29.3, and 11.3, respectively (Figs. 11 and 12), whereas E was allowed to vary. Best-fit parameters (±95% confidence interval) are shown in the corresponding plots. Data demonstrate that ethanol decreases allosteric parameter E. n = 4–8; each patch was excised from a different cell. Data are expressed as mean ± SEM.

would favor decreased (or at least reduced potentiation) cbv1+β1 channel activity by ethanol when compared with cbv1 channels. These modifications on gating are likely compounded by the fact that ethanol reduces E of cbv1+β1 heteromers but does not modify this parameter in cbv1 homomers (Tables 1 and 2). Thus, (a) quantitative differences on common gating processes and (b) unique disruption of coupling between Ca^{2+}_i binding and voltage sensor activation together very likely explain the fact that the steady-state channel activity of cbv1+β1 channels is inhibited, whereas that of cbv1 is activated in response to ethanol when evaluated at 3–20 µM Ca^{2+}_i (see also Discussion).

DISCUSSION

In spite of recent advances in our understanding of how ethanol at concentrations found in blood during moderate-heavy alcohol intoxication (50–100 mM) modulates BK channel activity and thus cell physiology, the gating mechanisms underlying such modulation remain unknown. All previous studies that addressed the response of BK currents to a brief (few minutes) exposure to ethanol in an alcohol-naive system, whether using recombinant slo1 proteins or native channels in their natural membrane environment, agreed that ethanol modulation of BK current occurred in the absence of perturbations in ion conduction or channel membrane expression (Brodie et al., 2007; Dopico et al., 2014). Thus, acute ethanol action on slo1 channel–mediated ionic current seems to be limited to that of a gating modifier. However, all studies previous to the present work have evaluated ethanol's overall effect on slo1 macroscopic current, open channel probability, and/or dwell time distributions under a limited range of stimulus conditions. Previous studies offer no clue on the specific gating processes targeted by ethanol that lead to modification of slo1 current.

In addition, several groups have documented that different auxiliary BK β subunits condition the overall response of the BK channel complex to intoxicating levels of ethanol. Thus, at physiological Ca^{2+}_i levels, homomeric slo1, heteromeric slo1+β4, and native neuronal channels thought to consist of slo1 and/or slo1+β4 subunits (Dopico et al., 1998; Martin et al., 2004; Liu et al., 2008; Wynne et al., 2009) are activated by 50–100 mM ethanol. In contrast, heteromeric slo1+β1 and native cerebral artery myocyte BK channels thought to consist of slo1+β1 subunits are usually inhibited under similar voltage and Ca^{2+}_i conditions (Liu et al., 2004; Bukiya et

Table 1. **Summary of best-fit parameters obtained for homomeric BK channel in the presence or absence of 50 mM ethanol**

Parameter	Control	50 mM ethanol
L_0	$2.3 \times 10^{-6} \pm 6.3 \times 10^{-7}$	$2.1 \times 10^{-6} \pm 2.8 \times 10^{-7}$
z_L	0.34 ± 0.05	0.35 ± 0.04
$V_h(J)$	155	154.1 ± 2.7
z_J	0.60 ± 0.04	0.57 ± 0.02
D	19.0 ± 1.39	19.1 ± 0.61
K_d	9.02 ± 1.4	1.0 ± 0.07
C	6.07 ± 0.1	4.7 ± 0.12
E	6.15 ± 2.1	6.3 ± 1.7

Table 2. **Summary of best-fit parameters obtained for β1-contianing BK channel in the presence or absence of 50 mM ethanol**

Parameter	Control	50 mM ethanol
L_0	$1.25 \times 10^{-7} \pm 4.4 \times 10^{-8}$	$1.3 \times 10^{-7} \pm 3.9 \times 10^{-8}$
z_L	0.41 ± 0.06	0.42 ± 0.03
$V_h(J)$	80	80.83 ± 1.6
z_J	0.60 ± 0.03	0.59 ± 0.02
D	30.2 ± 3.7	29.3 ± 2.62
K_d	19.0 ± 2.4	11.3 ± 1.2
C	27.2 ± 2.3	13.5 ± 0.45
E	9.5 ± 1.6	4.06 ± 0.55

al., 2009a). Moreover, ethanol-induced inhibition of cerebral artery myocyte BK channels is totally blunted by genetic ablation of β1 subunits (Bukiya et al., 2009a). Like ethanol, β subunits are gating modifiers; the actions of several of these accessory proteins on specific aspects of BK (slo1) channel gating (intrinsic gating–, voltage-, and Ca^{2+}_i-dependent parameters) are an expanding field of investigation (Cox and Aldrich, 2000; Bao and Cox, 2005; Orio and Latorre, 2005; Sweet and Cox, 2009; Contreras et al., 2012; Sun et al., 2013; Castillo et al., 2015). As found for studies of ethanol action on slo1 channels themselves, all previous studies on ethanol modulation of slo1+β heteromers have been limited to the descriptive electrophysiological approaches mentioned above. More importantly, these studies have been conducted using different slo1 isoforms, Ca^{2+}_i levels, expression systems, and/or membrane lipid composition, all factors that perturb slo1 channel gating by themselves (reviewed by Brodie et al., 2007; Dopico et al., 2012, 2014; Bettinger and Davies, 2014). This heterogeneity in experimental conditions makes it impossible to even determine the actual contribution (if any) of a given β subunit type to the overall effect of ethanol on BK current, not to mention identification of the underlying gating processes leading to such effect. To resolve these uncertainties and gaps in knowledge on ethanol–BK channel interactions, we systematically addressed the following questions: (a) whether ethanol indeed differentially modulates BK channels that differ only in β subunit type composition (i.e., cbv1±β1/wt β2/β2-IR/β3 d variant/β4) when studied under identical conditions using the same expression system and (b) which specific gating processes that control BK channel activity are distinctly modified by ethanol. This exploration was conducted within the framework of the HA allosteric model of channel gating (Horrigan and Aldrich, 1999, 2002; Horrigan et al., 1999; Bao and Cox, 2005; Orio and Latorre, 2005) by using a wide range of voltages and Ca^{2+} concentrations. We focused this analysis on homomeric cbv1 versus heteromeric cbv1+β1 channels because (a) ethanol exerts opposite effects on these currents (activation vs. inhibition) when evaluated within 3–20 µM Ca^{2+}_i and (b) the consequences of these differential ethanol effects have been well-documented: inhibition of neuronal firing in nucleus accumbens medium spiny neurons (Martin et al., 2004, 2008) and nociceptive DRG neurons (Gruß et al., 2001) versus constriction of cerebral arteries (Liu et al., 2004). Thus, addressing the distinct gating processes differentially targeted by ethanol in these constructs may likely provide mechanistic insights on alcohol-induced modification of excitable tissue physiology; (c) all other heteromeric BK channel combinations seem to follow the overall ethanol response of either homomeric cbv1 or heteromeric cbv1+β1 (see below). Throughout our experiments, we used an ethanol concentration (50 mM) reached in blood during moderate to heavy alcohol intoxication and widely reported to alter BK current and thus cell physiology (Liu et al., 2008; Bukiya et al., 2009a).

Present data demonstrate that the overall ethanol effect on BK channels that differ in β subunit composition when evaluated in the same system under the same recording conditions and including the same slo1 subunit (cbv1) does differ. At first glance, however, steady-state currents mediated by all constructs under study are markedly increased by ethanol when studied at low Ca^{2+}_i concentrations (<1 µM). This potentiation gradually decreases as Ca^{2+}_i increases until inhibition of current is reached (at >30 M Ca^{2+}_i). However, a closer inspection reveals two different phenotypes of overall ethanol effect on BK channel activity: the homomeric slo1 type (shared by cbv1, cbv1+β3 variant d, and cbv1+β4) and the slo1+β1 type (shared by cbv1+β1, cbv1+wt β2, and cbv1+β2-IR). The former is defined by a crossover in overall ethanol effect on current from activation to inhibition that occurs at ∼20 µM Ca^{2+}, whereas the latter is defined by such crossover being shifted to 3 µM Ca^{2+}_i. This change in crossover along the Ca^{2+}_i axis is critical because it implies that at activating levels of Ca^{2+}_i reached in excitable tissues in the vicinity of the BK channel (3–20 µM; Pérez et al., 2001), ethanol will increase BK current in the former while inhibiting current in the latter. Indeed, these outcomes have been reported with native BK channels thought to consist of slo1+β4 versus slo1+β1 subunits (Liu et al., 2004; Martin et al., 2004, 2008; Bukiya et al., 2009a).

A second major finding from probing ethanol on the steady-state current mediated by the different constructs is that ethanol's overall effect is identical in wt β2– and β2-IR–containing BK channels, indicating that the inactivation domain of wt β2 does not play a major role in the overall effect of the drug on steady-state activity. It should be stressed, however, that under our recording conditions (steady-state activity), the Po of slo1+wt β2 channels is dominated by the equilibrium between inactivated states and noninactivating states, and thus, obtaining gating parameters straightforwardly from the HA model is not tenable for this construct.

Gating analysis and fitting to the HA model of our data uncovered several important findings on ethanol actions on slo1 channels in the presence and absence of regulatory β subunits. First, ethanol's overall effect on BK current, whether defined by the slo1 or the slo1+β1 prototype described above (third paragraph of Discussion; see also Figs. 2 and 3), occurs in the absence of modification of the conformational change associated with the closed to open transition of the channel (e.g., L_0 and z_L remain unmodified). Thus, intrinsic gating remains conserved in the presence of ethanol levels that modify steady-state current. Second, ethanol fails to modify cbv1 $V_h(J)$, a parameter that has been widely used as an estimate of voltage sensor movement when

the channel is closed (Horrigan and Aldrich, 1999; Horrigan et al., 1999; Orio and Latorre, 2005). In addition, we demonstrated that the gating charge associated with each voltage sensor's movement (z_J) and the allosteric coupling factor between voltage sensor activation and channel opening (D) remained unchanged for both the slo1 and slo1+β1 prototypes. Finally, previous descriptive electrophysiology on mslo1 channels showed that 50–100 mM ethanol (a) failed to alter the rate-limiting slope of the ln NPo-V relationship and, thus, the effective valence (z; Dopico et al., 1998) and (b) similarly affected the $V_{0.5}$-Ca^{2+} versus $V_{0.5} \times Q$-Ca^{2+}_i plots of mslo1 channels (Liu et al., 2008). Collectively, present determinations from HA modeling and previous findings strongly argue that ethanol perturbs BK channel function in the absence of noticeable changes in voltage sensor function.

Our current data also showed that at Ca^{2+}_i <2 µM (which includes physiological Ca^{2+}_i found in excitable tissues), ethanol's response of the slo1 channel prototype is potentiation of steady-state current. This effect is related to a drastic increase in the channel's apparent Ca^{2+}_i binding affinity (K_d for Ca^{2+}_i decreases nine times in the presence of ethanol). The HA analysis also reveals that the ethanol effect on cbv1 current is an ∼20% decrease in allosteric coupling between Ca^{2+} binding and channel opening (C). At physiological Ca^{2+} levels (≤20 µM), the overall ethanol effect is potentiation of slo1 channel activity, which is explained by the drastic decrease in K_d caused by the alcohol. In a previous study, we used an ad hoc, very simple eight-state single-channel model (at constant voltage) to postulate that ethanol-induced inhibition of mslo1 current was caused by ethanol-induced facilitation of channel entry into a low Po mode triggered by nonphysiological, high Ca^{2+} (Liu et al., 2008). The specific gating parameter or parameters leading to this phenomenon were undetermined. From fitting data to Eq. 5 (Fig. 9), however, we now clearly demonstrate that the mild but significant decrease in BK Po evoked by ethanol at high Ca^{2+}_i is caused by the 20% decrease in C evoked by the alcohol.

Extending an early finding on mslo1 channels probed with ethanol in the presence of 1 mM Mg^{2+}_i and nominal zero Ca^{2+}_i (Liu et al., 2008), our current data unequivocally demonstrate that, in the absence of Ca^{2+}_i, cbv1 channels are insensitive to ethanol (Fig. S1) even when Mg^{2+}_i was present at sufficient levels (100 mM) to directly gate slo1 channels and increase BK current in the absence of Ca^{2+}_i (Fig. S1; Shi et al., 2002). These results, the fact that only Ca^{2+}-dependent parameters in the HA model (K_d and C) are ethanol-sensitive, and previous findings documenting the inability of ethanol to modulate ionic current mediated by other members of the slo channel family whose gating is driven by ions other than Ca^{2+}_i (i.e., slo2 and slo3) while the Ca^{2+}-gated MthK channel retains ethanol sensitivity (Liu et al., 2013) indicate that ethanol's overall effect on slo1 currents is specifically linked to Ca^{2+}_i-driven gating.

The combination of electrophysiology and computational methods provides some structural insights on the Ca^{2+} dependence of ethanol effect on slo1 currents. Combined amino acid substitutions that abolish Ca^{2+}_i sensing by the two high-affinity sites mapped to the slo1 protein CTD (i.e., the RCK2 high-affinity site and the D362,D367 site) abolish the channel's ethanol sensitivity (Liu et al., 2008). Equivalent mutations on a human slo1 gene introduced to *Caenorhabditis elegans* blunt ethanol-induced intoxication (Davis et al., 2015). In contrast, the same mutations on each high-affinity Ca^{2+} site, whether in mslo1, cslo1, or hslo1 in *C. elegans*, fail to blunt ethanol action on slo1 channels (Liu et al., 2008; Davis et al., 2015). Therefore, slo1 channels remain activatable by ethanol as far as Ca^{2+}_i is able to interact with either of the Ca^{2+}_i high-affinity sites in the slo1 CTD (for further discussion, see Liu et al. [2008]).

We have recently identified in the mslo1 CTD a pocket site of discrete dimensions where ethanol docks and increases Po. This site is fully conserved in cbv1 (which has a 99% identity with mslo1) and includes K361, which must hydrogen bond with ethanol for the alcohol to increase channel activity (Bukiya et al., 2014). Thus, the ethanol recognition site is adjacent to the RCK1 high-affinity Ca^{2+}_i-binding site determined by D362 and D367. Ligand-binding sites for ethanol and Ca^{2+}_i in slo1 channels are nearby but do not overlap (Liu et al., 2008; Bukiya et al., 2014), which makes alcohol and Ca^{2+}_i heterotropic ligands of BK channel–forming proteins. The close spatial location of ethanol and Ca^{2+} recognition, however, suggests that channel conformational changes upon binding of these two ligands (Ca^{2+}_i and ethanol) interact or converge to modulate overall channel activity. Remarkably, the ethanol pocket includes R514, a residue that participates in Ca^{2+}_i sensing (Schreiber and Salkoff, 1997; Shi et al., 2002; Zhang et al., 2010; Bukiya et al., 2014). Thus, R514 may serve as a structural link for ethanol action on slo1 channels being allosterically coupled to Ca^{2+}_i binding. Consistently, mslo1-K361N, R514N, mslo1-R514N channels display both resistance to ethanol and disrupted Ca^{2+}_i sensitivity. Moreover, in the Ca^{2+}_i-unbound state, ethanol is unable to hydrogen bond with K361, a chemical interaction that is necessary for ethanol to increase mslo1 channel activity; in the Ca^{2+}-free condition, R514 is shifted far away from the ethanol interaction, making it impossible for this residue to stabilize the K361–ethanol interaction (Bukiya et al., 2014). This model provides an explanation for the requirement of Ca^{2+}_i for ethanol to modulate slo1 activity as shown here with cbv1 (Fig. 2 and Fig. S1) and previously with mslo1 channels (Liu et al., 2008, 2013). The overall ethanol response of BK channels may also be determined by long-range interactions between the

ethanol and Ca^{2+}-binding sites and other regulatory slo1 domains. For example, CamKII-dependent phosphorylation of Thr107 in the S0–S1 cytosolic linker of bslo1 channels (from bovine aorta) blunts ethanol activation and favors ethanol inhibition of channel activity (Liu et al., 2006). The structural bases underlying functional cross-talking upon ethanol/Ca^{2+} binding to the slo1 CTD and CamKII interaction with bslo1 Thr107 remain unknown. It should be noted, however, that Thr107 is substituted by nonphosphorylatable residues in mslo1, hslo1, and rslo1, including cbv1 (used in our current study).

Modulation of ethanol effect on slo1-mediated currents by Mg^{2+}_i may have pathophysiological implications as alcoholics have reduced levels of Mg^{2+}_i (Marrero et al., 2015). A very recent study demonstrated that ethanol's effect on hslo1 currents expressed in HEK cells, as well as on native BK current in isolated hippocampal neurons, is modulated by Mg^{2+}_i. However, this modulation is lost in the presence of cytochalasin D, an actin destabilizer (Marrero et al., 2015). These data are consistent with the hypothesis that Mg^{2+}_i levels do not participate in directly modulating ethanol actions on slo1 channels. Indeed, our present data obtained across a wide Mg^{2+}_i range (0–100 mM) unequivocally demonstrated that Mg^{2+}_i, even when probed at levels that can gate slo1 channels in the absence of Ca^{2+}_i, does not empower the cbv1 channels with ethanol sensitivity as Ca^{2+}_i does. Consistently, previous data have demonstrated that mutations of the low-affinity Mg^{2+}-sensing mslo1 site (Glu374 and Glu399, which are conserved in cbv1) do not prevent ethanol from potentiating mslo1 channel activity (Liu et al., 2008). Collectively, data discussed so far indicate that ethanol modulation of slo1 channel gating is coupled to Ca^{2+} binding to this ion's high-affinity sites in the slo1 protein CTD but not to ion binding to the slo1 channel's low-affinity site for divalents.

As found for homomeric cbv1 channels, the HA model reveals that the gating processes of cbv1+β1 channels targeted by ethanol are linked to Ca^{2+}-binding gating, whereas intrinsic gating itself and major parameters of voltage gating under study remain unaltered in the presence of the alcohol (see Results section and Figs. 7, 8, 9, 10, 11, 12, and 13). However, within a wide Ca^{2+} range (3–20 µM) that includes physiological levels of Ca^{2+}_i in contracting vascular myocytes (Pérez et al., 2001), ethanol's overall effect is inhibition of steady-state current for constructs that follow the cbv1+β1 prototype. Thus, HA analysis unveils key distinctions in the gating processes targeted by ethanol in cbv1+β1 when compared with the homomeric slo1 prototype. First, ethanol also increases the channel's apparent Ca^{2+}_i sensitivity, yet this increase (two times when compared with the value in the absence of ethanol) is significantly smaller than that observed with homomeric cbv1 (nine times). Second, ethanol-induced decrease in C is larger for cbv1+β1 than for cbv1: −33% versus −20%. In addition, ethanol significantly decreases the E parameter in cbv1+β1 (−55%) yet does not modify E in homomeric cbv1. Collectively, a reduced increment in Ca^{2+}_i binding affinity of the unliganded channel in addition to reduced coupling between Ca^{2+}_i binding and channel opening as well as between Ca^{2+}_i binding and voltage sensor activation (Table 2) are gating determinants leading to decreased slo1+β1 channel activity in the presence of ethanol.

The HA analyses of our data underscore the limitation of descriptive electrophysiology in interpreting ethanol action and mechanisms on BK channels: an inspection of $V_{0.5}$ versus Ca^{2+}_i plots seems to indicate that at Ca^{2+}_i >2 µM, ethanol and β1 have opposite effects on cbv1 currents (Fig. 1 B vs. Fig. 3 D). Thus, ethanol could have been described as having an "anti–BK β1 action," with possible mechanistic speculations (e.g., the drug alters slo1–β1 coupling). Rather, HA analyses of our data demonstrate that (a) for both slo1 and slo1+β1 channels, intrinsic gating remains unperturbed by ethanol; (b) ethanol targets common gating parameters in slo1 and slo1+β1 channels (K_d and C), yet to a different degree: ethanol quantitative differences on the gating of these constructs very likely contribute to the differential ethanol effect on these channels when evaluated at physiological levels of Ca^{2+}_i; (c) ethanol's differential effect on slo1 and slo1+β1 channels also results from a qualitative difference in ethanol modification of channel gating: the alcohol significantly decreases the E parameter in the latter but not in the former.

The structural bases of β1 modulation of ethanol action on slo1 channels remain speculative mainly because neither the structural basis of slo1 modulation by ethanol (Bettinger et al., 2012; Bettinger and Davies, 2014; Bukiya et al., 2014) nor the structural bases of slo1 and β1 subunit interaction (Wallner et al., 1996; Orio and Latorre, 2005; Morrow et al., 2006; Wu et al., 2009, 2013; Gruslova et al., 2012; Kuntamallappanavar et al., 2014; Castillo et al., 2015) are fully resolved. Thus, we can speculate on several, albeit not mutually exclusive, possibilities: (a) ethanol interaction with the newly identified ethanol-sensing site (slo1 "activation site"; Bukiya et al., 2014) in slo1 CTD itself facilitates ethanol-induced inhibition when β1 subunits are present; (b) slo1 contains additional ethanol recognition sites that mediate a decrease in Po and become increasingly functional in the slo1-β1–coupled heteromer. Interestingly, the nicotinic acetylcholine receptor provides a precedent for a single protein containing distinct n-alkanol recognition sites: one mediating activation and the other inhibiting (Borghese et al., 2014). (c) The β1 subunit itself possesses an ethanol recognition/interaction site or sites, which favor channel inhibition upon ethanol binding; (d) finally, we cannot exclude the possibility that the presence of β1 subunits alters the chan-

nel's lipid microenvironment, known to regulate ethanol action on BK channels (reviewed in Dopico et al. [2014]).

BK β subunits have been widely reported to determine the basal BK current response to modulators, and several pharmacodynamics patterns have been described (Latorre and Contreras, 2013; Dopico et al., 2014; Torres et al., 2014). The chemotherapeutic agent tamoxifen and some endogenous lipids (17β-estradiol, cholane steroids, leukotrienes, and docosahexaenoic acids) require the presence of β1 subunits to increase BK channel steady-state activity (Valverde et al., 1999; Dick et al., 2001). In contrast, β1 subunits are not necessary for but amplify channel steady-state enhancement by phosphatidylinositol bisphosphate (PIP2; Vaithianathan et al., 2008). Accessory subunit-driven pharmacological selectivity has also been reported: corticosterone potentiates β4-containing BK channels but not slo1+wt β2 heteromers, whereas dehydroepiandrosterone potentiates the activity of slo1+wt β2 but not that of slo1+β4 channels (King et al., 2006). Current data underscore that accessory β subunits are not necessary for ethanol to modulate slo1-mediated currents, as previously shown (Liu et al., 2006, 2008; Martin et al., 2008). However, a new and more complex pharmacodynamics pattern emerges, in which β1 and wt β2 subunits favor a decrease in steady-state activity of BK current by ethanol and thus alter the prevalent ethanol response of homomeric slo1, whereas β3 or β4 subunit–containing heteromers respond to ethanol as homomeric slo1 does. Thus, different β subunits condition different qualitative responses of the BK channel to the same pharmacological agent.

In conclusion, our study documents for the first time that, at physiological Ca^{2+}_i levels, different β subunits are responsible for different ethanol responses of the same slo1 channels studied in the same expression system and under identical recording conditions. Thus, we unveiled two channels' ethanol response prototypes: slo1 type and slo1+β1 type, which are, respectively, activated and inhibited when probed with ethanol at physiological levels of Ca^{2+}_i. Moreover, HA analysis revealed the specific gating parameters that contribute to the differential ethanol effect of ethanol on these two BK channel prototypes. Our functional approaches, together with recent (Bukiya et al., 2014) and upcoming work addressing the structural bases of ethanol action on BK channels, may lead to designing new agents that target distinct regions in slo1 and/or BK β subunits and/or ethanol-sensitive, specific gating processes in order to oppose ethanol-induced modification of physiology.

ACKNOWLEDGMENTS

Authors thank Bangalore Shivakumar and Maria T. Asuncion-Chin for excellent technical assistance, Jianxi Liu and Phanindra Velisettyfor troubleshooting with some molecular biology procedures, and Anna N. Bukiya (University of Tennessee Health Science Center, Memphis, TN) for helpful discussion.

This work was supported by the American Heart Association Predoctoral Fellowship 13PRE14690014 (to G. Kuntamallappanavar) and National Institutes of Health grants R37AA11560 and R01HL104631 (to A.M. Dopico).

The authors declare no competing financial interests.

Richard W. Aldrich served as editor.

Submitted: 18 March 2016
Accepted: 14 October 2016

REFERENCES

Bao, L., and D.H. Cox. 2005. Gating and ionic currents reveal how the BK_{Ca} channel's Ca^{2+} sensitivity is enhanced by its β1 subunit. *J. Gen. Physiol.* 126:393–412. http://dx.doi.org/10.1085/jgp.200509346

Behrens, R., A. Nolting, F. Reimann, M. Schwarz, R. Waldschütz, and O. Pongs. 2000. hKCNMB3 and hKCNMB4, cloning and characterization of two members of the large-conductance calcium-activated potassium channel beta subunit family. *FEBS Lett.* 474:99–106. http://dx.doi.org/10.1016/S0014-5793(00)01584-2

Bettinger, J.C., and A.G. Davies. 2014. The role of the BK channel in ethanol response behaviors: evidence from model organism and human studies. *Front. Physiol.* 5:346. http://dx.doi.org/10.3389/fphys.2014.00346

Bettinger, J.C., K. Leung, M.H. Bolling, A.D. Goldsmith, and A.G. Davies. 2012. Lipid environment modulates the development of acute tolerance to ethanol in *Caenorhabditis elegans*. *PLoS One.* 7:e35192. http://dx.doi.org/10.1371/journal.pone.0035192

Borghese, C.M., J.A. Hicks, D.J. Lapid, J.R. Trudell, and R.A. Harris. 2014. $GABA_A$ receptor transmembrane amino acids are critical for alcohol action: disulfide cross-linking and alkyl methanethiosulfonate labeling reveal relative location of binding sites. *J. Neurochem.* 128:363–375. http://dx.doi.org/10.1111/jnc.12476

Brenner, R., T.J. Jegla, A. Wickenden, Y. Liu, and R.W. Aldrich. 2000a. Cloning and functional characterization of novel large conductance calcium-activated potassium channel β subunits, hKCNMB3 and hKCNMB4. *J. Biol. Chem.* 275:6453–6461. http://dx.doi.org/10.1074/jbc.275.9.6453

Brenner, R., G.J. Peréz, A.D. Bonev, D.M. Eckman, J.C. Kosek, S.W. Wiler, A.J. Patterson, M.T. Nelson, and R.W. Aldrich. 2000b. Vasoregulation by the β1 subunit of the calcium-activated potassium channel. *Nature.* 407:870–876. http://dx.doi.org/10.1038/35038011

Brodie, M.S., A. Scholz, T.M. Weiger, and A.M. Dopico. 2007. Ethanol interactions with calcium-dependent potassium channels. *Alcohol. Clin. Exp. Res.* 31:1625–1632. http://dx.doi.org/10.1111/j.1530-0277.2007.00469.x

Bukiya, A.N., J. Liu, L. Toro, and A.M. Dopico. 2007. β_1 (*KCNMB1*) subunits mediate lithocholate activation of large-conductance Ca^{2+}-activated K^+ channels and dilation in small, resistance-size arteries. *Mol. Pharmacol.* 72:359–369. http://dx.doi.org/10.1124/mol.107.034330

Bukiya, A.N., J. Liu, and A.M. Dopico. 2009a. The BK channel accessory β_1 subunit determines alcohol-induced cerebrovascular constriction. *FEBS Lett.* 583:2779–2784. http://dx.doi.org/10.1016/j.febslet.2009.07.019

Bukiya, A.N., T. Vaithianathan, L. Toro, and A.M. Dopico. 2009b. Channel β2–4 subunits fail to substitute for β1 in sensitizing BK

channels to lithocholate. *Biochem. Biophys. Res. Commun.* 390:995–1000. http://dx.doi.org/10.1016/j.bbrc.2009.10.091

Bukiya, A.N., J.E. McMillan, A.L. Fedinec, S.A. Patil, D.D. Miller, C.W. Leffler, A.L. Parrill, and A.M. Dopico. 2013. Cerebrovascular dilation via selective targeting of the cholane steroid-recognition site in the BK channel β1-subunit by a novel nonsteroidal agent. *Mol. Pharmacol.* 83:1030–1044. http://dx.doi.org/10.1124/mol.112.083519

Bukiya, A.N., G. Kuntamallappanavar, J. Edwards, A.K. Singh, B. Shivakumar, and A.M. Dopico. 2014. An alcohol-sensing site in the calcium- and voltage-gated, large conductance potassium (BK) channel. *Proc. Natl. Acad. Sci. USA.* 111:9313–9318. http://dx.doi.org/10.1073/pnas.1317363111

Castillo, K., G.F. Contreras, A. Pupo, Y.P. Torres, A. Neely, C. González, and R. Latorre. 2015. Molecular mechanism underlying β1 regulation in voltage- and calcium-activated potassium (BK) channels. *Proc. Natl. Acad. Sci. USA.* 112:4809–4814. http://dx.doi.org/10.1073/pnas.1504378112

Contreras, G.F., A. Neely, O. Alvarez, C. Gonzalez, and R. Latorre. 2012. Modulation of BK channel voltage gating by different auxiliary β subunits. *Proc. Natl. Acad. Sci. USA.* 109:18991–18996. http://dx.doi.org/10.1073/pnas.1216953109

Cox, D.H., and R.W. Aldrich. 2000. Role of the β1 subunit in large-conductance Ca^{2+}-activated K^+ channel gating energetics. Mechanisms of enhanced Ca^{2+} sensitivity. *J. Gen. Physiol.* 116:411–432. http://dx.doi.org/10.1085/jgp.116.3.411

Crowley, J.J., S.N. Treistman, and A.M. Dopico. 2003. Cholesterol antagonizes ethanol potentiation of human brain BK_{Ca} channels reconstituted into phospholipid bilayers. *Mol. Pharmacol.* 64:365–372. http://dx.doi.org/10.1124/mol.64.2.365

Crowley, J.J., S.N. Treistman, and A.M. Dopico. 2005. Distinct structural features of phospholipids differentially determine ethanol sensitivity and basal function of BK channels. *Mol. Pharmacol.* 68:4–10.

Davis, S.J., L.L. Scott, G. Ordemann, A. Philpo, J. Cohn, and J.T. Pierce-Shimomura. 2015. Putative calcium-binding domains of the *Caenorhabditis elegans* BK channel are dispensable for intoxication and ethanol activation. *Genes Brain Behav.* 14:454–465. http://dx.doi.org/10.1111/gbb.12229

Dick, G.M., C.F. Rossow, S. Smirnov, B. Horowitz, and K.M. Sanders. 2001. Tamoxifen activates smooth muscle BK channels through the regulatory beta 1 subunit. *J. Biol. Chem.* 276:34594–34599. http://dx.doi.org/10.1074/jbc.M104689200

Dopico, A.M. 2003. Ethanol sensitivity of BK_{Ca} channels from arterial smooth muscle does not require the presence of the β_1-subunit. *Am. J. Physiol. Cell Physiol.* 284:C1468–C1480. http://dx.doi.org/10.1152/ajpcell.00421.2002

Dopico, A.M., V. Anantharam, and S.N. Treistman. 1998. Ethanol increases the activity of Ca^{++}-dependent K^+ (mslo) channels: functional interaction with cytosolic Ca^{++}. *J. Pharmacol. Exp. Ther.* 284:258–268.

Dopico, A.M., A.N. Bukiya, and A.K. Singh. 2012. Large conductance, calcium- and voltage-gated potassium (BK) channels: regulation by cholesterol. *Pharmacol. Ther.* 135:133–150. http://dx.doi.org/10.1016/j.pharmthera.2012.05.002

Dopico, A.M., A.N. Bukiya, and G.E. Martin. 2014. Ethanol modulation of mammalian BK channels in excitable tissues: molecular targets and their possible contribution to alcohol-induced altered behavior. *Front. Physiol.* 5:466. http://dx.doi.org/10.3389/fphys.2014.00466

Glantz, S.A. 2001. Primer of Biostatistics. Fifth edition. McGraw-Hill, New York. 489 pp.

Gruslova, A., I. Semenov, and B. Wang. 2012. An extracellular domain of the accessory β1 subunit is required for modulating BK channel voltage sensor and gate. *J. Gen. Physiol.* 139:57–67. http://dx.doi.org/10.1085/jgp.201110698

Gruß, M., M. Henrich, P. König, G. Hempelmann, W. Vogel, and A. Scholz. 2001. Ethanol reduces excitability in a subgroup of primary sensory neurons by activation of BK_{Ca} channels. *Eur. J. Neurosci.* 14:1246–1256. http://dx.doi.org/10.1046/j.0953-816x.2001.01754.x

Horrigan, F.T., and R.W. Aldrich. 1999. Allosteric voltage gating of potassium channels II. Mslo channel gating charge movement in the absence of Ca^{2+}. *J. Gen. Physiol.* 114:305–336. http://dx.doi.org/10.1085/jgp.114.2.305

Horrigan, F.T., and R.W. Aldrich. 2002. Coupling between voltage sensor activation, Ca^{2+} binding and channel opening in large conductance (BK) potassium channels. *J. Gen. Physiol.* 120:267–305. (published erratum appears in *J. Gen. Physiol.* 2002. 120:599) http://dx.doi.org/10.1085/jgp.20028605

Horrigan, F.T., J. Cui, and R.W. Aldrich. 1999. Allosteric voltage gating of potassium channels I. Mslo ionic currents in the absence of Ca^{2+}. *J. Gen. Physiol.* 114:277–304. http://dx.doi.org/10.1085/jgp.114.2.277

Hoshi, T., A. Pantazis, and R. Olcese. 2013. Transduction of voltage and Ca^{2+} signals by Slo1 BK channels. *Physiology (Bethesda).* 28:172–189. http://dx.doi.org/10.1152/physiol.00055.2012

Jaggar, J.H., V.A. Porter, W.J. Lederer, and M.T. Nelson. 2000. Calcium sparks in smooth muscle. *Am. J. Physiol. Cell Physiol.* 278:C235–C256.

Jaggar, J.H., A. Li, H. Parfenova, J. Liu, E.S. Umstot, A.M. Dopico, and C.W. Leffler. 2005. Heme is a carbon monoxide receptor for large-conductance Ca^{2+}-activated K^+ channels. *Circ. Res.* 97:805–812. http://dx.doi.org/10.1161/01.RES.0000186180.47148.7b

King, J.T., P.V. Lovell, M. Rishniw, M.I. Kotlikoff, M.L. Zeeman, and D.P. McCobb. 2006. β2 and β4 subunits of BK channels confer differential sensitivity to acute modulation by steroid hormones. *J. Neurophysiol.* 95:2878–2888. http://dx.doi.org/10.1152/jn.01352.2005

Knaus, H.G., K. Folander, M. Garcia-Calvo, M.L. Garcia, G.J. Kaczorowski, M. Smith, and R. Swanson. 1994. Primary sequence and immunological characterization of β-subunit of high conductance Ca^{2+}-activated K^+ channel from smooth muscle. *J. Biol. Chem.* 269:17274–17278.

Kuntamallappanavar, G., L. Toro, and A.M. Dopico. 2014. Both transmembrane domains of BK β1 subunits are essential to confer the normal phenotype of β1-containing BK channels. *PLoS One.* 9:e109306. http://dx.doi.org/10.1371/journal.pone.0109306

Latorre, R., and G. Contreras. 2013. Keeping you healthy: BK channel activation by omega-3 fatty acids. *J. Gen. Physiol.* 142:487–491. http://dx.doi.org/10.1085/jgp.201311100

Ledoux, J., M.E. Werner, J.E. Brayden, and M.T. Nelson. 2006. Calcium-activated potassium channels and the regulation of vascular tone. *Physiology (Bethesda).* 21:69–78. http://dx.doi.org/10.1152/physiol.00040.2005

Liu, J., M. Asuncion-Chin, P. Liu, and A.M. Dopico. 2006. CaM kinase II phosphorylation of slo Thr107 regulates activity and ethanol responses of BK channels. *Nat. Neurosci.* 9:41–49. http://dx.doi.org/10.1038/nn1602

Liu, J., T. Vaithianathan, K. Manivannan, A. Parrill, and A.M. Dopico. 2008. Ethanol modulates BK_{Ca} channels by acting as an adjuvant of calcium. *Mol. Pharmacol.* 74:628–640. http://dx.doi.org/10.1124/mol.108.048694

Liu, J., A.N. Bukiya, G. Kuntamallappanavar, A.K. Singh, and A.M. Dopico. 2013. Distinct sensitivity of slo1 channel proteins to ethanol. *Mol. Pharmacol.* 83:235–244. http://dx.doi.org/10.1124/mol.112.081240

Liu, P., Q. Xi, A. Ahmed, J.H. Jaggar, and A.M. Dopico. 2004. Essential role for smooth muscle BK channels in alcohol-

induced cerebrovascular constriction. *Proc. Natl. Acad. Sci. USA*. 101:18217–18222. http://dx.doi.org/10.1073/pnas.0406096102

Lu, R., A. Alioua, Y. Kumar, M. Eghbali, E. Stefani, and L. Toro. 2006. MaxiK channel partners: physiological impact. *J. Physiol.* 570:65–72. http://dx.doi.org/10.1113/jphysiol.2005.098913

Marrero, H.G., S.N. Treistman, and J.R. Lemos. 2015. Ethanol effect on BK channels is modulated by magnesium. *Alcohol. Clin. Exp. Res.* 39:1671–1679. http://dx.doi.org/10.1111/acer.12821

Martin, G., S. Puig, A. Pietrzykowski, P. Zadek, P. Emery, and S. Treistman. 2004. Somatic localization of a specific large-conductance calcium-activated potassium channel subtype controls compartmentalized ethanol sensitivity in the nucleus accumbens. *J. Neurosci.* 24:6563–6572. http://dx.doi.org/10.1523/JNEUROSCI.0684-04.2004

Martin, G.E., L.M. Hendrickson, K.L. Penta, R.M. Friesen, A.Z. Pietrzykowski, A.R. Tapper, and S.N. Treistman. 2008. Identification of a BK channel auxiliary protein controlling molecular and behavioral tolerance to alcohol. *Proc. Natl. Acad. Sci. USA*. 105:17543–17548. http://dx.doi.org/10.1073/pnas.0801068105

McManus, O.B., L.M. Helms, L. Pallanck, B. Ganetzky, R. Swanson, and R.J. Leonard. 1995. Functional role of the β subunit of high conductance calcium-activated potassium channels. *Neuron.* 14:645–650. http://dx.doi.org/10.1016/0896-6273(95)90321-6

Morrow, J.P., S.I. Zakharov, G. Liu, L. Yang, A.J. Sok, and S.O. Marx. 2006. Defining the BK channel domains required for β1-subunit modulation. *Proc. Natl. Acad. Sci. USA*. 103:5096–5101. http://dx.doi.org/10.1073/pnas.0600907103

Nelson, M.T., and J.M. Quayle. 1995. Physiological roles and properties of potassium channels in arterial smooth muscle. *Am. J. Physiol.* 268:C799–C822.

Nimigean, C.M., and K.L. Magleby. 2000. Functional coupling of the β_1 subunit to the large conductance Ca^{2+}-activated K^+ channel in the absence of Ca^{2+}. Increased Ca^{2+} sensitivity from a Ca^{2+}-independent mechanism. *J. Gen. Physiol.* 115:719–736. http://dx.doi.org/10.1085/jgp.115.6.719

Orio, P., and R. Latorre. 2005. Differential effects of β1 and β2 subunits on BK channel activity. *J. Gen. Physiol.* 125:395–411. http://dx.doi.org/10.1085/jgp.200409236

Orio, P., P. Rojas, G. Ferreira, and R. Latorre. 2002. New disguises for an old channel: MaxiK channel β-subunits. *News Physiol. Sci.* 17:156–161.

Palacio, S., C. Velázquez-Marrero, H.G. Marrero, G.E. Seale, G.A. Yudowski, and S.N. Treistman. 2015. Time-dependent effects of ethanol on BK channel expression and trafficking in hippocampal neurons. *Alcohol. Clin. Exp. Res.* 39:1619–1631. http://dx.doi.org/10.1111/acer.12808

Pérez, G.J., A.D. Bonev, and M.T. Nelson. 2001. Micromolar Ca^{2+} from sparks activates Ca^{2+}-sensitive K^+ channels in rat cerebral artery smooth muscle. *Am. J. Physiol. Cell Physiol.* 281:C1769–C1775.

Qian, X., and K.L. Magleby. 2003. β1 subunits facilitate gating of BK channels by acting through the Ca^{2+}, but not the Mg^{2+}, activating mechanisms. *Proc. Natl. Acad. Sci. USA*. 100:10061–10066. http://dx.doi.org/10.1073/pnas.1731650100

Salkoff, L., A. Butler, G. Ferreira, C. Santi, and A. Wei. 2006. High-conductance potassium channels of the SLO family. *Nat. Rev. Neurosci.* 7:921–931. http://dx.doi.org/10.1038/nrn1992

Schreiber, M., and L. Salkoff. 1997. A novel calcium-sensing domain in the BK channel. *Biophys. J.* 73:1355–1363. http://dx.doi.org/10.1016/S0006-3495(97)78168-2

Shi, J., G. Krishnamoorthy, Y. Yang, L. Hu, N. Chaturvedi, D. Harilal, J. Qin, and J. Cui. 2002. Mechanism of magnesium activation of calcium-activated potassium channels. *Nature.* 418:876–880. http://dx.doi.org/10.1038/nature00941

Sun, X., J. Shi, K. Delaloye, X. Yang, H. Yang, G. Zhang, and J. Cui. 2013. The interface between membrane-spanning and cytosolic domains in Ca^{2+}-dependent K^+ channels is involved in β subunit modulation of gating. *J. Neurosci.* 33:11253–11261. http://dx.doi.org/10.1523/JNEUROSCI.0620-13.2013

Sweet, T.B., and D.H. Cox. 2008. Measurements of the BK_{Ca} channel's high-affinity Ca^{2+} binding constants: effects of membrane voltage. *J. Gen. Physiol.* 132:491–505. http://dx.doi.org/10.1085/jgp.200810094

Sweet, T.B., and D.H. Cox. 2009. Measuring the influence of the BK_{Ca} β1 subunit on Ca^{2+} binding to the BK_{Ca} channel. *J. Gen. Physiol.* 133:139–150. http://dx.doi.org/10.1085/jgp.200810129

Torres, Y.P., S.T. Granados, and R. Latorre. 2014. Pharmacological consequences of the coexpression of BK channel α and auxiliary β subunits. *Front. Physiol.* 5:383. http://dx.doi.org/10.3389/fphys.2014.00383

Uebele, V.N., A. Lagrutta, T. Wade, D.J. Figueroa, Y. Liu, E. McKenna, C.P. Austin, P.B. Bennett, and R. Swanson. 2000. Cloning and functional expression of two families of β-subunits of the large conductance calcium-activated K^+ channel. *J. Biol. Chem.* 275:23211–23218. http://dx.doi.org/10.1074/jbc.M910187199

Vaithianathan, T., A. Bukiya, J. Liu, P. Liu, M. Asuncion-Chin, Z. Fan, and A. Dopico. 2008. Direct regulation of BK channels by phosphatidylinositol 4,5-bisphosphate as a novel signaling pathway. *J. Gen. Physiol.* 132:13–28. http://dx.doi.org/10.1085/jgp.200709913

Valverde, M.A., P. Rojas, J. Amigo, D. Cosmelli, P. Orio, M.I. Bahamonde, G.E. Mann, C. Vergara, and R. Latorre. 1999. Acute activation of Maxi-K channels (*hSlo*) by estradiol binding to the β subunit. *Science.* 285:1929–1931. http://dx.doi.org/10.1126/science.285.5435.1929

Wallner, M., P. Meera, M. Ottolia, G.J. Kaczorowski, R. Latorre, M.L. Garcia, E. Stefani, and L. Toro. 1995. Characterization of and modulation by a beta-subunit of a human maxi KCa channel cloned from myometrium. *Receptors Channels.* 3:185–199.

Wallner, M., P. Meera, and L. Toro. 1996. Determinant for β-subunit regulation in high-conductance voltage-activated and Ca^{2+}-sensitive K^+ channels: an additional transmembrane region at the N terminus. *Proc. Natl. Acad. Sci. USA*. 93:14922–14927. http://dx.doi.org/10.1073/pnas.93.25.14922

Wallner, M., P. Meera, and L. Toro. 1999. Molecular basis of fast inactivation in voltage and Ca^{2+}-activated K^+ channels: a transmembrane β-subunit homolog. *Proc. Natl. Acad. Sci. USA*. 96:4137–4142. http://dx.doi.org/10.1073/pnas.96.7.4137

Weiger, T.M., A. Hermann, and I.B. Levitan. 2002. Modulation of calcium-activated potassium channels. *J. Comp. Physiol. A Neuroethol. Sens. Neural Behav. Physiol.* 188:79–87. http://dx.doi.org/10.1007/s00359-002-0281-2

Wu, R.S., N. Chudasama, S.I. Zakharov, D. Doshi, H. Motoike, G. Liu, Y. Yao, X. Niu, S.X. Deng, D.W. Landry, et al. 2009. Location of the β4 transmembrane helices in the BK potassium channel. *J. Neurosci.* 29:8321–8328. http://dx.doi.org/10.1523/JNEUROSCI.6191-08.2009

Wu, R.S., G. Liu, S.I. Zakharov, N. Chudasama, H. Motoike, A. Karlin, and S.O. Marx. 2013. Positions of β2 and β3 subunits in the large-conductance calcium- and voltage-activated BK potassium channel. *J. Gen. Physiol.* 141:105–117. http://dx.doi.org/10.1085/jgp.201210891

Wynne, P.M., S.I. Puig, G.E. Martin, and S.N. Treistman. 2009. Compartmentalized β subunit distribution determines characteristics and ethanol sensitivity of somatic, dendritic, and terminal large-conductance calcium-activated potassium channels in the rat central nervous system. *J. Pharmacol. Exp. Ther.* 329:978–986. http://dx.doi.org/10.1124/jpet.108.146175

Xia, X.M., J.P. Ding, and C.J. Lingle. 1999. Molecular basis for the inactivation of Ca^{2+}- and voltage-dependent BK channels in adrenal chromaffin cells and rat insulinoma tumor cells. *J. Neurosci.* 19:5255–5264.

Xia, X.M., J.P. Ding, and C.J. Lingle. 2003. Inactivation of BK channels by the NH_2 terminus of the β2 auxiliary subunit: An essential role of a terminal peptide segment of three hydrophobic residues. *J. Gen. Physiol.* 121:125–148. http://dx.doi.org/10.1085/jgp.20028667

Yuan, C., M. Chen, D.F. Covey, L.J. Johnston, and S.N. Treistman. 2011. Cholesterol tuning of BK ethanol response is enantioselective, and is a function of accompanying lipids. *PLoS One.* 6:e27572. http://dx.doi.org/10.1371/journal.pone.0027572

Zeng, X., X.M. Xia, and C.J. Lingle. 2008. Species-specific differences among KCNMB3 BK β3 auxiliary subunits: Some β3 N-terminal variants may be primate-specific subunits. *J. Gen. Physiol.* 132:115–129. http://dx.doi.org/10.1085/jgp.200809969

Zhang, G., S.Y. Huang, J. Yang, J. Shi, X. Yang, A. Moller, X. Zou, and J. Cui. 2010. Ion sensing in the RCK1 domain of BK channels. *Proc. Natl. Acad. Sci. USA.* 107:18700–18705. http://dx.doi.org/10.1073/pnas.1010124107